Trends and Zonal Variability of Extreme Rainfall Events Over East Africa During 1960-2017

Moses.A Ojara
Nanjing University of Information Science and Technology https://orcid.org/0000-0002-3989-3702
Yunsheng Lou (yunshlou@163.com)
Nanjing University of Information Science and Technology
Hasssen Babaousmail
Nanjing University of Information Science and Technology
Peter Wasswa
Makerere University

Research Article

Keywords: Rainfall extreme events, DFA, East Africa

Posted Date: March 4th, 2021

DOI: https://doi.org/10.21203/rs.3.rs-273628/v1

Trends and Zonal Variability of Extreme Rainfall events over East Africa during 1960-2017

Moses A. Ojara [1, 2, 3], Yunsheng Lou[1, 2*], Hasssen Babaousmail[1, 2], Peter Wasswa[4]

[1]Collaborative Innovation Center on Forecast and Evaluation of Meteorological Disasters, Nanjing University of Information Science and Technology, Nanjing 210044, China

[2]Jiangsu Key Laboratory of Agricultural Meteorology, College of Applied Meteorology, Nanjing University of Information Science and Technology, Nanjing 210044, China

[3]Uganda National Meteorological Authority, Plot 21, 28 Port Bell Rd, Kampala P.O. Box 7025 Kampala, Uganda.

[4]Makerere University College of Geoinformation, Environment and Climate Sciences

***Corresponding Author**

Prof. Dr Lou Yunsheng

Email:yunshlou@163.com

Abstract

East African countries (Uganda, Kenya, Tanzania, Rwanda, and Burundi) are prone to weather extreme events. In this regard; the past occurrence of extreme rainfall events is analyzed for 25 stations following the Expert Team on Climate Change Detection and Indices (ETCCDI) regression method. Detrended Fluctuation Analysis (DFA) is used to show the future development of extreme events. Pearson's correlation analysis is performed to show the relationship of extreme events between different rainfall zones and their association with El Niño -Southern Oscillation (ENSO and Indian Ocean dipole (IOD) IOD-DMI indices. Results revealed that the consecutive wet day's index (CWD) was decreasing trend in 72% of the stations analyzed, moreover consecutive dry days (CDD) index also indicated a positive trend in 44% of the stations analyzed. Heavy rainfall days index (R10mm) showed a positive trend at 52% of the stations and was statistically significant at a few stations. In light of the extremely heavy rainfall days (R25mm) index, 56% of the stations revealed a decreasing trend for the index and statistically significant trend at some stations. Further, a low correlation coefficient of extreme rainfall events in the regions; and between rainfall extreme indices with the atmospheric teleconnection indices (Dipole Mode Index-DMI and Nino 3.4) ($r = -0.1$ to $r = 0.35$). Most rainfall zones showed a positive correlation between the R95p index and DMI, while 5/8 of the rainfall zones experienced a negative correlation between Nino 3.4 index and the R95p. In light of the highly variable trends of extremes events, we recommend planning adaptation and mitigation measures that consider the occurrence of such high variability. Measures such as rainwater harvesting, stored and used during needs, planned settlement, and improved drainage systems management supported by accurate climate and weather forecasts is highly advised.

Keywords: ***Rainfall extreme events, DFA, East Africa***

1. Introduction

East African (EA) countries (Uganda, Kenya, Tanzania, Rwanda, and Burundi) are prone to climate and weather extreme events that usually expose their population to risks and vulnerability (Kilavi et al. 2018). The rains are highly variable and frequently associated with extremes events such as flash floods (Indeje et al. 2000; Nicholson 2017), and droughts (Gamoyo et al. 2015). These events continue to increase great stress on many EA countries by disrupting food production and distribution channels in the region (FAO 2017). The impact of some climate extreme events such as frequent flash floods, long dry spells, frequent droughts usually result in damages to socio-economic infrastructure, food insecurity, and loss of lives (Schlenker and Lobell 2010; Adhikari et al. 2015; Onyutha 2016; Pereira 2017). Extreme climate events have led to the human population suffering especially in the face of more frequent droughts and floods in the region (Lyon and DeWitt 2012).

Several parts of EA have experienced one or more extreme precipitation episodes over the last decades. For example; Uganda has experienced alternating episodes of floods, droughts, or dry spells in eastern and northeastern which have resulted in frequent loss of human lives, livestock, as well as the destruction of socio-economic infrastructure (Onyutha 2016). And according to the World Bank report of 2009, Kenya experienced financial loss worth 870 million dollars during 1997/1998 ENSO/ El Niño events that led to flooding in the region (Davis et al. 2009). Besides these; climate extremes events cause massive loss of life of other living organisms and threaten the total extinction of some vital species (Downing 1991; Omondi et al. 2013). Incidences of pests and disease occurrence with extreme climate events have been examined by other authors (e.g Pascal et al. 2006; Stern et al. 2011).

Seasonal rainfall over EA is also regulated by the weather phenomena such as the Indian Ocean dipole (IOD) (Behera et al. 2005; Onyutha 2016) and El Niño -Southern Oscillation (ENSO), which are associated with the interannual variability as well as extreme rainfall events (Indeje et al. 2000; Ogwang et al. 2015a; Onyutha 2016). For example; the warm phase of ENSO/ El Niño usually results in extremely high rainfall in most parts of EA which normally causes occasional floods like the episode of 1997/1998 (Amissah et al. 2002; Takaoka 2005). Conversely, the cold phase of ENSO/ La Niña is associated with extremely dry air and subsequently drought conditions of most regions of EA.

Standardized rainfall anomaly revealed an increase in the intensity of extreme precipitation events for above normal cases over EA (Ongoma et al. 2018), and the region is expected to strongly warm and rainfall extremes increased by the end of the twenty-first century (Ongoma et al. 2017). Results from recent global studies indicate changes in frequencies, intensity, geographical extent, duration, and timing of climate extreme events (Cai et al. 2014). An increase in rainfall extreme events such as very wet days

(R95p) and extremely wet days (R99p) predicted in the future (2021-2100) are bounds to cause the loss of lives and destruction of property due to increase in flood intensities and drought frequencies (Ongoma et al. 2017).

Moreover, incidences of upward tendencies in the length of the maximum dry spell occurring during rainy months have been reported in the region (Tilya and Mhita 2007; Ojara et al. 2020), which are associated with the reduction to crop production in the region. In addition to these, rainfall related extreme events such as; wet days, annual total precipitation in wet days (PRCPTOT), simple daily intensity index (SDII), heavy precipitation days, very heavy precipitation days, and severe precipitation, have recorded significant changes over the recent decades (Bouagila et al. 2013; Gitau et al. 2018; Ongoma et al. 2018).

A recent study suggests that the annual trends of precipitation indices such as the number of days with precipitation ≥20mm (R20mm), (R50mm), and very wet days of precipitation amounts (R95p) were generally decreasing from 1981 to 2010, but positive trends in the indices are revealed under representative concentration pathways (RCP4.5) future climate scenario (Nimusiima et al. 2019).

Considering the impacts of extreme rainfall events over EA which range from loss of human and animal lives to the destruction of properties, it is important to fully understand previous climate events and their impacts to make more accurate and reliable forecasts to alleviate their impact (Ogwang et al., 2015b; Onyutha 2016). While we acknowledge previous attempts aimed at generating information on extreme rainfall events over EA (e.g Hague 2010; Ogwang et al. 2015b; Ongoma and Chen 2018; Kilavi et al. 2018; Nimusiima et al. 2019; Nkunzimana et al. 2019), in-depth and regular comprehensive analysis of rainfall extremes events which are required to support adaptation and mitigation of impacts are still inadequate. The present study analyses daily observed rainfall data to show the recent past occurrence of extreme rainfall events and their consistency for future development in EA.

The remaining subsequent sections of the present study are structured as follows: Section 2 describes the study domain, datasets, and methods. This is followed by section 3 presenting the main results. Section 4 elucidates the conclusion and recommendations based on the findings of this research.

2 Data and Methodology

2.1 Study Area

The study domain is East Africa (EA) comprising 5 countries located in the eastern part of the African continent (Fig.1). The region is enclosed within the geographical latitudes 5.1° N to 11.74° S and longitudes 28.86° E to 41.91° E. The main physical features in the region include open water bodies, valleys, and high mountains with a maximum altitude of 5882 meters above sea level (Fig.1b).

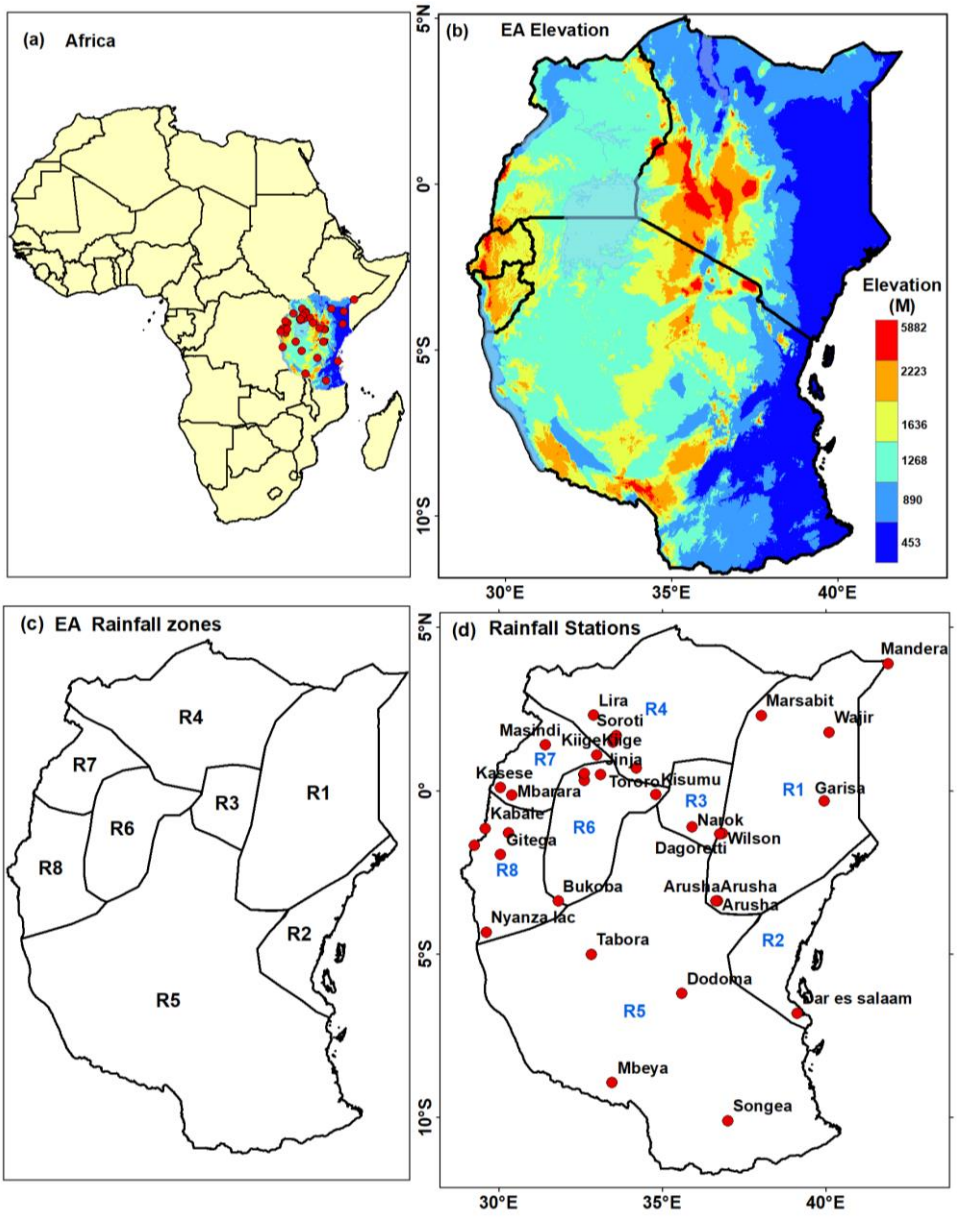

Fig.1: Shows map of Africa (a), showing East Africa right (b), and meteorological stations (red dots).

Normally; EA experiences two main rainy seasons; the first season occurs in months of March-April and May (MAM), usually referred to as the ''long rains'' (Camberlin and Philippon 2002; Gamoyo et al. 2015; Ogwang et al. 2016; Ongoma and Chen 2017), and this is frequently termed as the Borel spring. This season follows the Inter-tropical convergence zone (ITCZ) migration to the northern hemisphere, and the second season usually referred to as "short rains'' (Kizza et al. 2009) occurs during October to December (OND) resulting from the movement of the ITCZ from the north to Southern hemisphere. The rains are also influenced by atmospheric phenomena such as El-Nino Southern Oscillation (ENSO) (Indeje et al. 2000; Ntale and Gan 2004) and the Indian Ocean Dipole (IOD) (Behera

et al. 2005). The El Niño Southern Oscillation (ENSO) phenomena are strongly associated with the inter-annual variability of rainfall in this region (Indeje et al. 2000).

2.2 Data

2.2.1 In situ datasets

Daily and monthly rainfall datasets from meteorological agencies namely; Uganda National Meteorological Authority, Kenya Meteorological Department. Rwanda Meteorology Agency, and Geographical Institute of Burundi and Tanzania Meteorological Authority were sourced. Detail geographical and rainfall statistical information for each meteorological station are presented in table 1.

Table 1: Show the details of the Meteorological stations used in this study

Station name	Long (Deg)	Lat (Deg)	Elevation (Meters)	Data Period	Annual rainfall (mm) Min	Max	Mean	RF zone (R1-R8)
Wajir	41.9	3.9	271.0	1960-2016	80.5	1129.1	334.1	1
Garissa	40.1	1.8	246.1	1957-2016	102.9	369.8	208.1	1
Marsabit	38.0	2.3	1283.2	1960-2016	99.7	1469.4	725.0	1
DAR	39.1	-6.8	156.2	1980-2017	585.0	1990.2	1139.2	2
Dagoretti	36.8	-1.3	1830.0	1961-2016	258.1	1028.3	478.6	3
Narok	35.9	-1.1	1950.4	1964-2016	695.2	867.4	413.0	3
Namulonge	32.6	0.5	1128.1	1963-2017	676.3	1475.6	1120.0	4
Tororo	34.2	0.7	1176.2	1970-2017	1032.4	2160.4	1522.2	4
Soroti	33.6	1.7	1115.1	1961-2014	1011.1	1726.6	1347.6	4
Jinja	33.1	0.5	1175.0	1961-2017	914.0	1700.0	1286.9	4
Lira	32.9	2.3	1120.4	1971-2017	1106.3	1873.1	1501.7	4
Serere	33.5	1.5	1098.2	1961-2017	850.1	2380.2	1356.0	4
Kiige	33.0	1.1	1089.1	1971-2017	735.4	1968.3	1322.0	4
Bukoba	31.8	-3.4	1144.0	1960-2016	1523.6	2736.1	2071.4	5
Mbeya	33.5	-8.9	1791.5	1960-2017	617.4	1287.5	931.0	5
Kisumu	34.8	-0.1	1154.3	1960-2016	178.5	1366.4	936.1	6
Kampala	32.6	0.3	1162.2	1980-2016	223.4	1295.3	783.7	6
Entebbe	32.6	0.5	1117.7	1951-2016	271.7	1592.1	1073.1	6
Mbarara	30.4	-0.1	1408.3	1950-2016	183.4	933.2	451.3	7
Kasese	30.1	0.1	931.0	1964-2016	179.7	975.4	502.2	7
Masindi	31.4	1.4	1136.2	1960-2016	276.0	1298.7	445.1	7
Kabale	29.6	-1.2	1743.1	1960-2016	136.1	1039.6	745.6	8
Gitega	30.1	-2.0	1524.4	1970-2017	381.0	1129.1	413.3	8
Nyagatare	30.3	-1.3	1366.2	1970-2017	203.3	804.0	209.3	8
Nyanza lac	29.6	-4.3	874.0	1970-2017	192.1	1227.1	933.4	8
Gisenyi	29.3	-1.7	1591.8	1970-2017	193.0	995.4	589.1	8

The duration for all country datasets was taken varying from 1950 to 2017. The data was collected from manual rain gauges. The stations were selected to represent homogenous rainfall zones of EA

(Fig.1). Preliminary quality assessment of data at source includes; checks control to identify the negative precipitations values, typing errors to identify gaps in the dataset, false zeros. Thereafter statistical quality assessments were performed on the datasets as described in the methodology section.

2.1.3 Atmospheric Indices.

Two main climate indices are used to show the influence of major atmospheric indices on rainfall variability in EA. The indices were selected based on the relevancy demonstrated in past studies explaining the variation in rainfall over EA (Indeje et al. 2000; Behera et al. 2005; Onyutha 2016). First; the El Nino-Southern Oscillation (ENSO), Nino3.4 index which is of monthly temporal resolution represents the interaction between the atmosphere and the Ocean in the Tropical Pacific which periodically causes variation below-normal or above-normal sea surface temperatures and dry and wet conditions over a few years. ENSO climate index was accessed from the link;
https://www.esrl.noaa.gov/psd/gcos_wgsp/Timeseries/Data/nino34.long.anom.data

The IOD is the anomalous SST difference between the western (50°-70°E and 10°S-10°N) and south-eastern (90°-110°E and 10°S-0°N) of the Indian Ocean (Onyutha 2016). It is an interannual climate pattern exhibited across the tropical Indian Ocean (Saji et al.1999; Behera et al. 2005). Saji et al. (1999) suggest that cooler than normal water and warmer than normal water in the tropical western Indian Ocean characterizes the positive IOD period. On the other hand, a negative IOD period is shown by the positive conditions at the same location in the ocean. The monthly IOD time series data can be downloaded from the NOAA official website (https://www.esrl.noaa.gov). These two indices were selected based on the relevancy demonstrated in past studies explaining the variability of rainfall over EA (Indeje et al. 2000; Behera et al. 2005; Onyutha 2016).

2.1.4 Climate Hazards Group Infrared Precipitation with Stations datasets (CHIRPS)

To examine recent spatial variability in extreme events, the CHIRPS gridded dataset of high resolution (0.05°x 0.05°) for 1981 to date was selected. CHIRPS data is one of the best datasets compared to ground observation datasets that have been greatly used for variability studies in East Africa (e.g Gebrechorkos et al. 2019). Lack of well-distributed and managed rain-gauges in the region is a challenge to spatial analysis of climate data (Nicholson et al. 2018; Wainwright et al. 2019), which can only be overcome by the use of satellite or reanalysis datasets. This dataset was developed by merging three types of information of high resolution including global climatology, satellite estimates, and in situ observations, which greatly improved the rainfall products. More details of CHIPRPS data can be found

from Funk et al. (2015). The performances of Satellite dataset (CHIRPS) using statistical matrices such as correlation coefficient (R), root mean square error (RMSE) and Bias present a good representation of rainfall with station observations over the region except over a few areas (Table S2).

2.3. Methodology

2.3.1 Missing, Outlier, Normality and Homogeneity test

Some stations had few gaps which were filled based on the recommendation that data gaps can be filled if there are no more than 5 consecutive missing days or less than 10 days throughout the monthly data (WMO 2013). The estimation of missing data was performed using linear regression methods as it is simple to compute and gives good results (Kizza et al. 2009).

Outlier test was performed using Grubb's test and the results showed 2 outliers in Jinja stations which were found to be due to data entry error after verification with (WMO) form 49A for rainfall data entry. The remaining stations did not show outliers.

A normality test was performed using Shapiro-Wilk tests for the distribution type at a 5% significance level. All data were found to be approximately normally distributed. This was followed by the homogeneity test to ensure that variation in the climate data is due to climatic factors only (Aguilar et al. 2003). The test helps in avoiding wrong results leading to bias interpretations and conclusions about the data (Costa and Soares 2009). The data were tested for homogeneity using two methods; Standard normal homogeneity test (SNHT) and Buishand's test at a 5 % significant level. The null hypothesis was that the data were homogenous. Reference can be drawn from (Buishand 1982; Aguilar et al 2003) for a detailed discussion about the homogeneity test. This preliminary result is presented in Table S3.

2.3.4 Occurrence of extreme rainfall events.

Statistical metrics for analyzing extreme events in climate indices compiled by the Expert Team on Climate Change Detection Indices (ETCCDI) group have been computed. The method developed by the ETCCDI group to extract moderate climate indices is a regression approach. Typical of these climate indices are well described in (Zhang 2011; Sillmann et al. 2013), these tend to examine only "moderate event" in rainfall and are typically occurring at least once a year (Zhang et al. 2011). In total, 11 rainfall related indices from the ETCCDI lists were extracted using the RClimDex tool (Zhang et al. 2005). The most important factor with this tool is that it is designed to perform quality checks and data harmonization process before the actual analysis is done. The indices are deemed important for this study based on the literature analysis from other authors (Mubiru et al. 2012; Ongoma and Chen. 2017). Descriptions, code

200 names of each rainfall extreme indices are well-described (Table S1) and more detailed mathematical
201 expression can be obtained from the website for ETCCDI;
202 (http://etccdi.pacificclimate.org/list_27_indices.shtml).
203
204 **2.3.5 Relationship between extreme rainfall events with synoptic-scale teleconnections**
205 To show the relationship between extreme rainfall indices and two main synoptic-scale
206 teleconnections; ENSO and IOD within the 8 rainfall zones were established using a correlation
207 coefficient. First; rainfall data for each meteorological station in given rainfall zones were aggregated and
208 extreme rainfall indices were computed. Correlation analysis was perfumed to show the relationship
209 between extreme rainfall indices within any two given rainfall zones (R1-R8), as well as establish the
210 influence of two atmospheric indices (ENSO-Nino3.4) and Indian Ocean Dipole (DMI) in each of the
211 rainfall zones, Pearson's correlation analysis was performed and the correlation coefficient (r') plotted in
212 a correlation diagrams for some key rainfall indices

213 **2.3.6 Detrended fluctuation analysis (DFA)**

214 Detrended fluctuation analysis (DFA) is a correlation analysis based on a long-range power-law
215 method developed in recent years for the study of Deoxyribonucleic acid (DNA), but it is also suitable for
216 nonstationary time series (Peng et al. 1994). The development of DFA techniques have been accepted and
217 widely used in many studies of the long-range correlation in natural science and systems. For example; Li
218 and Zhang (2007) used the DFA method to quantify fraction dynamics of groundwater systems in a small
219 agricultural watershed and observed that fluctuations of groundwater levels and base flow are dynamic
220 responses of the groundwater system to its recharge e.tc,

221 Varotsos et al. (2006) used the same approach in the study of the global Aerosol Index (AI) to find
222 self-similarity properties in their values extracted from satellite measurement during 1979-2003. In more
223 directly related research, the approach was employed in the scaling of near-surface air temperature
224 fluctuations and its geographical distribution analyzed in the simulation of the current climate with a
225 complex atmosphere-ocean model (Fraedrich and Blender 2003). Recently; DFA techniques were used to
226 analyze the trends and extreme values in extreme temperature and precipitation events in Inner Mongolia
227 (China) during 1960–2017 by Tong et al. (2019)
228 In this study, DFA was used to predict future development trends in extreme climate indices. DFA
229 is computed following Step-wise procedure for calculation of trends in precipitation extremes (Tong et al.
230 2019), given below;

First, for precipitation sequence (x_k, k =1, 2… N), N is the length of the precipitation extreme sequence, $\bar{x}$ is the mean value, and the accumulative deviation sequence of the original sequence is determined by equation (1) below;

$$y(i)=\sum_{k-1}^{N}\left(x_k-\bar{x}\right), \text{ where; } (i=1,2,3.....N) \quad (1)$$

Thereafter, the new sequence y(i) was divided into Ns series of non-overlapping sub-intervals with a length of s:

$$N_s = int(\mathrm{N}/\mathrm{s}) \quad (2)$$

In this computation the sequence is not precisely divisible, thus to ensure the integrity of the information, the sequence is divided once more in the reverse direction so that a total of 2Ns sub-intervals could be obtained. The value of 's' was selected according to the length of the sequence and the operational requirements.

This was followed by a polynomial fitting on the data of each sub-interval v(v = 1, 2, ……..…2Ns), and a local trend function yv(i) was obtained. Then the trend of the original sequence is eliminated in the sub-function to strain out the trend in the sequence as ys(i)

$$\mathrm{y}_s(i)=y(i)-y_v(i) \quad (i=1,2,3.....N) \quad (3)$$

yv(i) can be first order, second order, or higher order polynomial; the second-order polynomial is used here. After the elimination of the trend, the variance in each interval was calculated as follows:

$$F^2(v,s)=\frac{1}{s}\sum_{i-1}^{s}\left\{y\left[(v-1)s+i\right]-y_v(i)\right\}^2 \quad (4)$$

, where $(i=1,2,3.....N)$

$$F^2(v,s)=\frac{1}{s}\sum_{i-1}^{s}\left\{y\left[N-(v-N_s)s+i\right]-y_v(i)\right\}^2 \quad (5)$$

and $(i=N_s+1,N_s+2,N_s+3.....2N_s)$

The second-order wave function of the whole sequence was determined as follows: Fs

$$\mathrm{F}(s)=\sqrt{\frac{1}{2N_s}\sum_{v-1}^{s}F^2(v,s)} \quad (6)$$

Finally, power-law correlations of F(s) and s changes were analyzed by the equation (7):

$$F(s): \ s^{a} \text{ or } \ln F(s) = a \ln s + b \quad (7)$$

In this double logarithmic coordinate, the data were fitted by the least square method and the slope 'a' of the linear trend is the scaled DFA index. If slope a = 0.5, shows that the sequence is random and is an independent random process. But, if 0 < a < 0.5, then the values of the sequence are not independent and therefore represent a short-range correlation or anti-persistence, which symbolizes that the data series has the opposite trend relative to that of the previous time series. However, if 0.5 < a < 1, then the process is continuous and the future trend is consistent with the previous trend. The closer the value is to 1, the greater the tendency of this consistency.

3. Results and Discussion

3.1 Normality and Homogeneity test.

The results of the homogeneity test using the Standard Normal Homogeneity Test (SNHT) showed that all the stations are approximately homogeneous, while the Buishand test at a 5% significance level shows that only 2 stations are inhomogeneous in 2 different months. These two stations are; Kotido and Nakasongola station were dropped from further analysis. Rainfall data for most stations in the region were also found to be homogenous (Mugume et al. 2016: Ongoma et al. 2018). Preliminary of this quality control analysis is presented in Table S2 at the Appendix.

3.3 Spatial distribution and trends of extreme rainfall events

Figure 3 shows the spatial distribution of 8 main rainfall indices over East Africa during the recent period (1981-2017). Results showed that the total number of rainy days index (Rn=1.0mm) in most parts of EA including rainfall zone 4,6,7 and Western Kenya towards Mount Elgon, experienced more numbers of rainy days ranging from 118 to 180 days in a year (Fig.3a). The number of rainy-day patterns shows a reduction towards the highlands of Rwanda, Burundi, and western Tanzania receiving about 91 to 118 days of rainfall. In reference to the pattern of consecutive dry days, (CDD) the entire Uganda, Rwanda and Burundi, Western Kenya to northwestern Kenya, Mountain Kenya areas (rainfall zone 3) extending to most parts of rainfall zone 2, and the coastal area along rainfall zone 5 experienced the lowest number of dry days (CDD) ranging from 17 to 91 days, while northeastern Kenya in rainfall zone 1(R1), and most of Southwestern, Western and Central parts of Tanzania, covering a large proportion of rainfall zone 5 (R5) received the highest number of CDD days ranging from 91 to 180 days (Fig.3b).

For heavy rainfall days (R10mm), a higher number of days (45-57 days) are observed to be concentrated around Lake Victoria and Mount Elgon, to most parts of northern Uganda, Southwestern Tanzania, and Burundi in rainfall zone 8. With exception of northern Kenya in rainfall zone1 which received less than 20 days of heavy rainfall days (R10mm), the majority of EA received about 18 to 37 days of heavy rainfall days (R10mm). (Fig.3c). The result indicated that the entire EA received less than 20 days (8 -18 days) of very heavy rainfall days (R20mm) during the period 1981-2017(Fig.3d).

Throughout the analysis (1981-2017), the highest rainfall amount in the one day (RX1day) range from 29.0 mm to 140.0 mm, the largest portion of EA showed a range of 29.0 to 80.0 mm. relatively higher values (68.8-140.0mm) are experienced in Mount Kenya located in rainfall zone 3, to the coast bordering the Indian Ocean (Fig.3e). A similar pattern is recorded for the highest rainfall amount in five consecutive days (Rx5day), however; the lowest amount of rainfall recorded for Rx5day is relatively higher than those from RX1day ranging 68.8-140.0mm (Fig.3f).

For a very wet day's index (R95p), the highest amount of rainfall (200-273.0 mm) is received in spots around lake Victoria and the coastal region bordering the Indian Ocean and southeastern Tanzania. The majority of EA received between 137.3 to 200.0 mm except the vast portion of ASAL and central Tanzania which received between 54.1 to 137.3 mm of rainfall (Fig.3g). Extremely wet days index (R99p) showed that a large part of EA had 54.1- 96.1mm, followed by 14.1-54.1 mm in the ASAL area and spot in central Tanzania, least by the highest values of 96.1- 137.3 mm in Lake Victoria and the coastal region bordering the Indian Ocean and southeastern Tanzania (Fig.3h).

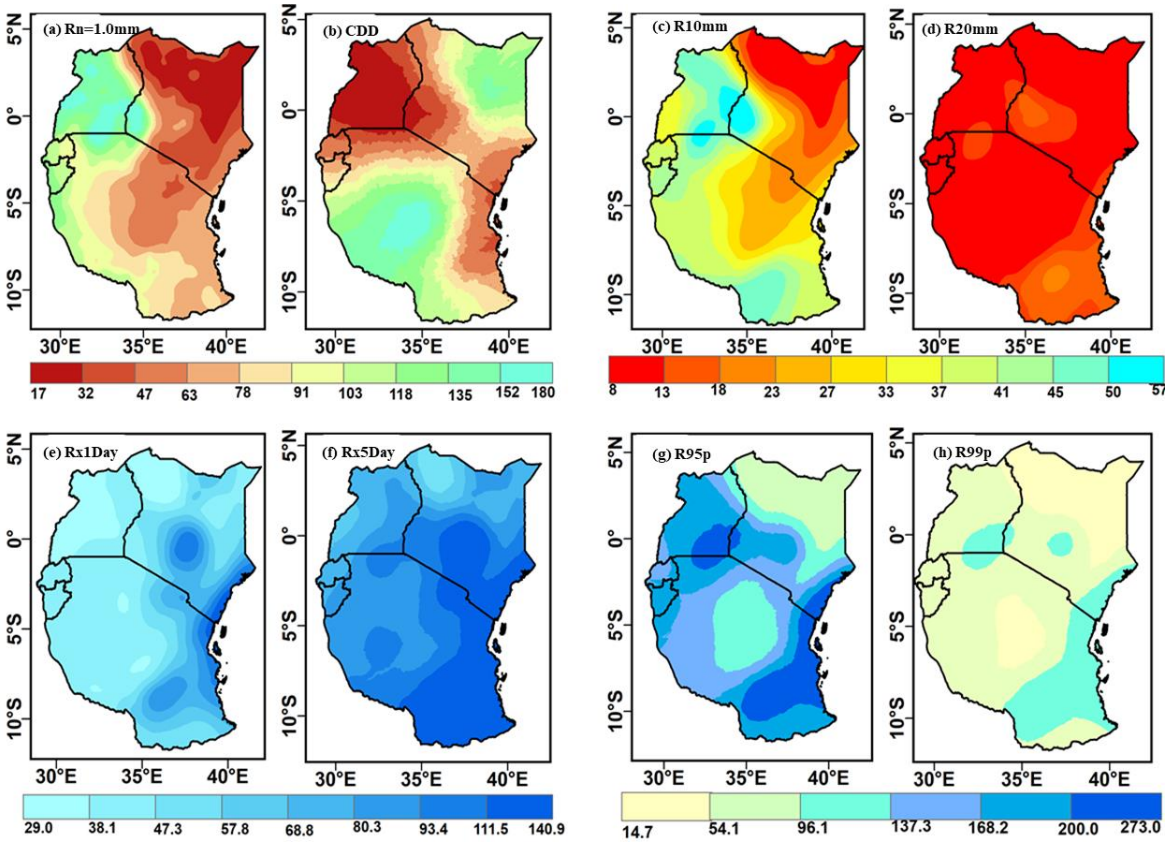

304

305 ***Fig.3. Shows the spatial distribution for the wet day (Rn=1.0mm(a), consecutive dry day CDD(b), the***
306 ***annual count of days when precipitation≥ 10mm(c), the annual count of days when precipitation≥ 20mm(d),***
307 ***max 5-day precipitation amount (RX1day) (e), 5-day precipitation amount (RX5day) (f), Very wet days R95p (g)***
308 ***and extremely wet days R95p (h) over East Africa during the period 1981-2017***

309

310 **3.4 Temporal trends of extreme rainfall events**

311 Table 2 represents the result of trends of rainfall extreme indices for different stations in EA based
312 on a varying period of 1960 to 2017. According to Alexander et al.,(2006), the first category of rainfall
313 indices that contains CDD, CWD, R10mm, R20mm, and R25mm are used to calculate the frequency of
314 the index exceeding or not exceeding its defined threshold. The CDD index measures dryness whereas the
315 CWD index directly represents a time-series relationship that relates to wetter conditions (Kiros et al.,
316 2017). The second class of Indices such as RX1day, RX5day, PRCPTOT, SDII, R95P, and R99P is used
317 to measure the rainfall depth in millimeter or intensity of rainfall in millimeter per day (Alexander et
318 al.,2006; Kiros et al., 2017).

319 In the first category, the analysis of consecutive dry days (CDD) index was able to detect a
320 positive trend in 44% (11/45) of the stations analyzed. These were found to be statistically significant

trends at 3 stations including; Wajir station in the Arid and Semi-Arid region (ASAL) of Kenya in rainfall zone (R11), Serere station in rainfall zone 4 (R4), and Mbeya station in rainfall zone 5(R5). In each case, the rate of increase was; 0.7 days/year, 0.4 days/year, and 0.61 days/year respectively. The increasing tendencies of CDD in the first regions (R1) corresponds to the decreasing trends in precipitation recently reported (Mumo et al., 2019), while for the second rainfall zone (R4), the drying pattern has been observed (Mubiru et al., 2012; Kansiime et al., 2013). Similarly; the length of maximum dry spells is revealed to be significantly increased in rainfall zone 4 (R4) over the last 2 decades (Ojara et al., 2020).

The consecutive wet day's index (CWD) shows a decreasing trend in 72% (18/25) of the stations analyzed and the trend is statistically significant for Garissa, DAR, and Lira and Mbeya stations in the rainfall zone 1, 2, 4, and 5 respectively. For the few stations (28%) (7/25) that indicated a positive pattern in the CWD index, only the Kisumu station in the rainfall 6 showed a statistically significant trend for the index. The increasing trend of CDD and decreasing trend in CWD in the Greater Horn of Africa (GHA) has also been observed by other recent studies (Omondi et al. 2013). EA is reported to be experiencing a decreasing trend in precipitation especially in the main season) (Lyon and Dewitt 2012; Rowell et al. 2015), which is most likely that indices related to precipitation measure will show such a negative trend.

Additionally, heavy rainfall days (R10mm) show a positive trend at 52% (13/25) of the stations but the trend is statistically significant at only 3 stations; Jinja, Kisumu, and Kasese stations each increasing at a rate of 0.11 days/year, 0.15 day/year, and 0.142 days/year respectively. The remaining 48% (12/25) stations portrayed an insignificance positive trend for the (R10mm) index. Among the stations which revealed a negative trend for heavy rainfall days (R10mm) index; only the Gitega station in rainfall zone 8 showed statistical significance results with a rate of change of -0.365mm/year. Similar results have been observed by other authors linking such an incidental trend to the changing climate in EA (Ongoma et. al 2018). Contrary to this, 60% (15/25) of the stations analyzed revealed a statistical insignificance positive trend for very heavy rainfall days (R20mm) index, and 40% (10/25) indicated a negative trend in the R20mm index with two stations; Kisumu and Entebbe in rainfall zone 6 showing a statistically significant decreasing trend at similar rates of -0.146 day/year and -0.168 day/year respectively.

Similarly; extremely heavy rainfall days (R25mm) revealed a decreasing trend in 56%1(4/25) of the stations. Stations such as Kisumu, Entebbe showed a statistically significant trend with a rate of decrease of -0.164mm/year, -0.129mm/year, and -0.157 mm/year respectively. The very heavy rainfall days (R20mm) and extremely heavy rainfall days (R25mm) index are associated to flash floods in the region (Ongoma and Chen 2018).

353 Rainfall indices related to the depth or intensity of rainfall including; (RX1day, RX5day, SDII,
354 R95P R99P, and PRCPTOT also show varied results. The results show that the index; the highest rainfall
355 amount in the one-day (RX1day) was decreasing trend in 40% (10/25) stations and the trends were
356 statistically significant at Wajir; Kisumu, Bukoba, and Entebbe station. The rates of decrease of rainfall in
357 these stations were; -0.59 mm/year, -0.72mm/year, -0.54 mm/year respectively. Besides, rainfall indices
358 showing the highest rainfall amount in five consecutive days (Rx5day) showed a decreasing trend in 36%
359 (9/25) stations but the trend is statistically significant at Entebbe, changing at a rate of -0.95 mm/year. In
360 this case; the remaining 64% (16/25) of the stations revealed positive trends but statistically significant at
361 Dar-es-salaam (DAR) and Jinja stations; each increasing at the rate of 2.06 mm/year and 0.39 mm/year.
362 Simple daily intensity index (SDII) indicated positive trends 60% (15/25) of stations with stations
363 like Namulonge, Jinja, Tororo, Serere in rainfall zone 4, and Kabale stations in rainfall 8 showing a
364 statistically significant trend. SDII index was observed to be changing at s rate of -0.042 to 0.62 mm/year
365 between stations. Stations like Namulonge, Jinja, and Kabale are located within the Lake Victoria basin
366 were found to show the highest increase in SDII values (Ongoma and Chen 2018). SDII revealed a
367 decreasing trend in 40% (10/25) of the stations analyzed, and statistically significant negative trends are
368 observed at Entebbe and Gitega stations, each changing at -0.031mm/year, and -0.042 mm/year
369 respectively.
370 Regarding the trend of very wet days (R95p); 60% (15/25) of the stations showed an increasing
371 trend with 4 stations; Dar-es-salaam (DAR), Tororo, Jinja, and Lira showed statistically significant
372 positive trends, increasing at; 9.57 mm/year, 3.53 mm/year, 5.1mm/year, and 4.96 mm/year respectively
373 (Table 2). The last 3 stations; Tororo, Jinja, and Lira are located in the low-lying area of lake Kyoga Basin
374 in Uganda which is prone to high frequent flask floods and drought events in recent decades (Onyutha
375 2016). The remaining 40% (10/25) stations indicated a negative trend in the very wet day's (R95p) index;
376 but the most notable stations with a significant statistical trend include; Kisumu; Entebbe. For these 3
377 stations; the rates of decrease in (R95p) index over period of analysis are; -4.03 mm/year, -3.06 mm/year;
378 -5.29 mm/year respectively.
379 Besides; (R99p) indicated a negative trend in 52% (13/25) stations although only one station
380 (Entebbe station) was statistically significant while the remaining 48% (12/25) of the stations showed an
381 increasing tendency for the trend of extremely wet days (R99p), but a significant statistical at some few
382 stations such as Tororo, Jinja, and Lira station. The rate of change at these stations was; 2.24 mm/year,
383 3.1mm/year, and 2.77 mm/year respectively (Table 2).

Finally, the index wet-day annual total rainfall (PRCPTOT), 60% (15/25) of the stations showed positive trends in the total annual precipitation, and 2 stations Kampala, Jinja, Kiige, and Kasese stations were statistically significant; increasing at 6.75 mm/year, 12.87 mm/year, and 4.52 mm/year respectively. For the remaining 40% (12/25) of stations which indicated a negative trend; only Gitega station was found to be statistically significantly decreasing at the rate of -7.23 mm/year.

Results of trends of extreme rainfall events in EA have shown varied results for different indices analyzed for each rainfall zones. This showed the natural heterogeneity of the rainfall in the region that is brought about by much complex association of large-scale controls variables like topography, lakes, and the maritime influence, and seasonal dynamics of tropical circulation, etc. (Nicholson 2017). Generally, the indices showed both negative and positive trends which are either statistically significant or insignificant throughout the analysis, which is in a closed agreement with other studies of extremes in the region (Omondi et al., 2013; Ongoma et al. 2018; Nkunzimana et al. 2019). The most notable negative results have been revealed in consecutive wet day's index (CWD) which showed a decreasing trend in 72% (18/25) of the stations analyzed especially in rainfall zone 1(R1) covering parts of north and northeastern Kenya where a reduction in rainfall have been proven (Mumo et al. 2019 and East and northeastern Uganda where rainfall reduction with occasional floods have been reported (Mubiru et al. 2012; Nimusiima et al., 213).

Simple daily intensity index (SDII) indicated a positive change and was statistically significant on many occasions, perhaps the anticipated pronouncement of the intensity of precipitation in tropical regions as a result of the global warming is now coming to foreplay (Owor et al. 2009), which need to be proven.

Table 2a: Shows the trends in climatic extreme indices of rainfall for 25 Meteorological stations and eight rainfall zones (R1-R8) in East Africa. The bold and shaded p-values (P-V) indicate statistically significant trends for the index and Q= Sen's' slope for the rate of change at a 5% significance level.

Stations		Rx1day	Rx5day	SDII	R10	R20	R25	CDD	CWD	R95P	R99P	PRCP TOT
Wajir	Q	-0.59	-0.40	-0.04	-0.03	-0.03	-0.02	0.68	-0.01	-1.30	-0.88	-1.73
	P-V	**0.04**	0.35	0.31	0.52	0.35	0.46	**0.01**	0.52	0.15	0.10	0.26
Garissa	Q	0.20	-0.21	0.06	-0.14	-0.06	-0.40	0.60	-0.04	-0.10	0.71	-10.82
	P-V	0.44	0.65	0.30	0.13	0.18	**0.00**	0.11	**0.02**	0.91	0.13	0.25
DAR	Q	2.09	2.06	0.23	-0.09	0.14	-0.56	-0.16	-0.11	9.57	3.59	45.87
	P-V	**0.00**	**0.03**	**0.00**	0.40	0.07	**0.00**	0.17	**0.02**	**0.01**	0.06	0.07
Dagoretti	Q	0.29	-0.01	0.13	-0.01	0.01	0.03	0.06		1.13	-0.07	-1.46
	P-V	0.25	0.99	**0.00**	0.83	0.89	0.39	0.56	0.08	0.40	0.91	0.50
Narok	Q	0.01	-0.31	0.04	-0.06	-0.01	-0.01	-0.02	-0.04	-0.95	-0.49	-2.47
	P-V	0.96	0.22	**0.03**	0.41	0.82	0.82	0.84	0.18	0.33	0.32	0.17
Namulonge	Q	0.08	0.11	0.05	0.03	0.06	0.08	0.11	-0.03	1.74	0.54	0.57
	P-V	0.58	0.66	**0.01**	0.74	0.14	**0.03**	0.13	0.19	0.16	0.45	0.76
Tororo	Q	0.30	0.42	0.05	0.06	0.06	0.10	0.18	-0.08	3.53	2.24	3.74
	P-V	0.18	0.09	**0.01**	0.44	0.27	**0.01**	0.10	0.49	**0.05**	**0.04**	0.13
Soroti	Q	0.20	0.14	0.01	-0.02	0.00	-0.02	0.10	0.01	0.99	1.10	-0.34
	P-V	0.18	0.52	0.61	0.68	0.90	0.46	0.40	0.70	0.38	0.08	0.82
Jinja	Q	0.25	0.39	0.05	0.11	0.15	0.05	-0.03	-0.03	5.10	3.10	5.13
	P-V	0.14	**0.02**	**0.01**	**0.05**	0.26	0.39	0.55	0.55	0.01	**0.00**	**0.05**
Lira	Q	0.13	0.02	-0.01	0.02	0.03	0.05	-0.23	-0.10	4.96	2.77	4.53
	P-V	0.65	0.97	0.55	0.84	0.68	0.39	0.41	**0.01**	**0.01**	**0.04**	0.11
Serere	Q	-0.16	0.05	-0.01	-0.08	-0.06	-0.05	0.39	0.02	-1.41	-0.50	-3.41
	P-V	0.28	0.84	0.62	0.29	0.28	0.35	**0.04**	0.51	0.34	0.54	0.13
Kiige	Q	1.18	0.90	0.07	0.44	0.27	0.24	-0.25	-0.16	7.18	3.42	12.87
	P-V	0.09	0.27	0.42	0.09	0.19	0.12	0.53	0.20	0.17	0.22	0.05
Mbeya	Q	-0.02	0.16	0.03	-0.01	0.09	-0.36	0.61	-0.18	1.52	-0.16	-0.49
	P-V	0.88	0.61	0.12	0.93	0.16	**0.05**	**0.01**	**0.01**	0.25	0.82	0.79
Bukoba	Q	-0.72	0.32	-0.01	0.12	0.03	0.27	-0.24	-0.07	-2.41	-1.57	2.26
	P-V	**0.01**	0.57	0.62	0.45	0.73	0.22	**0.03**	0.08	0.32	0.27	0.46
Kisumu	Q	-0.54	-0.35	-0.02	0.15	-0.15	-0.16	0.07	0.10	-4.03	-1.11	1.87
	P-V	**0.01**	0.36	**0.06**	**0.04**	**0.00**	**0.00**	0.35	**0.00**	**0.00**	0.14	0.25
Kampala	Q	-0.31	0.22	-0.03	0.18	0.01	-0.03	-0.10	0.04	0.30	-0.32	6.75
	P-V	0.34	0.59	0.15	0.10	0.96	0.74	0.40	0.57	0.90	0.82	**0.05**
Entebbe	Q	-0.85	-0.95	-0.03	-0.02	-0.17	-0.13	-0.02	-0.01	-3.06	-1.48	-2.66
	P-V	**0.00**	**0.00**	**0.01**	0.69	**0.00**	**0.00**	0.74	0.69	**0.01**	**0.05**	0.13
Mbarara	Q	-0.03	0.13	0.01	-0.02	0.04	0.04	0.08	-0.01	1.02	0.43	0.02
	P-V	0.79	0.50	0.09	0.70	0.15	0.06	0.64	0.31	0.17	0.36	0.99
Kabale	Q	0.05	0.03	0.03	0.07	-0.01	-0.01	-0.09	-0.03	0.43	0.29	0.90
	P-V	0.69	0.86	**0.00**	0.20	0.72	0.57	0.53	0.12	0.56	0.51	0.42
Kasese	Q	-0.20	-0.01	0.03	0.14	-0.07	-0.03	-0.15	0.03	-1.18	-0.14	4.52
	P-V	0.18	0.97	0.10	**0.05**	0.18	0.30	0.47	0.18	0.28	0.82	**0.01**
Masindi	Q	0.25	0.17	0.01	0.11	0.05	0.05	-0.19	-0.02	1.02	-0.26	2.94
	P-V	0.35	0.59	0.20	0.13	0.39	0.17	0.17	0.34	0.39	0.69	0.18
Gitega	Q	-0.28	-0.21	-0.04	-0.37	-0.17	-0.16	0.24	0.15	-5.29	-0.93	-7.23
	P-V	0.22	0.57	**0.02**	**0.00**	0.13	**0.04**	0.46	0.34	**0.05**	0.45	**0.01**
Nyagatare	Q	0.17	0.20	0.01	0.02	0.02	0.05	-0.25	-0.06	2.04	1.12	0.80
	P-V	0.43	0.59	0.52	0.88	0.75	0.25	0.42	0.25	0.19	0.25	0.81
Nyanza lac	Q	0.13	-0.13	-0.02	-0.17	-0.08	-0.05	-0.12	-0.06	-1.90	-0.80	-3.60
	P-V	0.61	0.75	0.25	0.20	0.21	0.42	0.78	0.61	0.27	0.38	0.23
Gisenyi	Q	0.50	0.51	-0.01	0.10	0.05	0.06	-0.33	0.07	2.47	1.51	4.12
	P-V	0.12	0.13	0.52	0.41	0.28	0.09	0.32	0.53	0.12	0.22	0.17

Table 2a: Shows the trends in climatic extreme indices for average rainfall for eight rainfall zones (R1-R8) in East Africa

R1	Q	-0.19	-0.31	0.01	-0.08	-0.04	-0.21	0.64	-0.03	-0.70	-0.08	-6.28
	P-V	0.24	0.50	0.30	0.32	0.26	0.23	0.06	0.27	0.53	0.12	0.26
R2	Q	2.09	2.06	0.23	-0.09	0.14	-0.56	-0.16	-0.11	9.57	3.59	45.87
	P-V	**0.00**	**0.03**	**0.00**	0.40	0.07	**0.00**	0.17	**0.02**	**0.01**	0.06	0.07
R3	Q	0.15	-0.16	0.08	-0.04	0.00	0.01	0.02	-0.04	0.09	-0.28	-1.96
	P-V	0.62	0.11	**0.04**	0.20	0.41	0.43	0.45	0.07	0.73	0.12	0.33
R4	Q	0.37	0.45	0.14	0.16	0.14	0.15	-0.03	0.02	3.81	2.10	4.50
	P-V	0.30	0.48	**0.03**	0.45	0.39	0.25	0.31	0.38	0.16	0.02	0.29
R5	Q	-0.02	0.16	0.03	-0.01	0.09	-0.36	0.61	-0.18	1.52	-0.16	-0.49
	P-V	0.88	0.61	0.12	0.93	0.16	**0.05**	**0.01**	**0.01**	0.25	0.82	0.79
R6	Q	-0.57	-0.36	-0.03	0.10	-0.10	-0.11	-0.02	0.04	-2.26	-0.97	1.99
	P-V	**0.05**	0.18	**0.03**	0.36	**0.00**	**0.00**	0.55	0.35	**0.01**	0.10	0.19
R7	Q	0.03	0.08	0.02	0.12	-0.01	0.01	-0.17	0.01	-0.08	-0.20	3.73
	P-V	0.27	0.78	0.15	0.13	0.28	0.23	0.32	0.26	0.34	0.76	0.18
R8	Q	0.27	0.19	-0.01	-0.01	0.00	0.02	-0.23	-0.02	0.87	0.61	0.44
	P-V	0.39	0.49	0.43	0.50	0.41	0.26	0.51	0.46	0.19	0.28	0.40

Implications of such trends of extreme rainfall events are most likely to be diverse as both positive and negative trends have been revealed from the analysis in different regions. For instance, regions such as northeastern Kenya in the rainfall zone 1(R1) which showed negative trends in CWD, PRCPTOT, and a positive trend in CDD are most likely to suffer socioeconomic hardship as agriculture will probably going to be affected by such trend. Measures for improving water availability and management such as rainwater harvesting, stored and used for crops and livestock are possibly the best options for these regions. Conversely; there are possibilities of other areas experiences continued flooding as a result of an increase in indices such as R25mm, R95p, R99p, and PRCPTOT as in rainfall zone 4 (R4) already reported (Barasa et al. 2015). This is also common in hilly areas of rainfall zone 8 like in Kigali as it has been reported to cause economic loss (Tsinda et al. 2014). Urban cities like Nairobi, Kampala, etc, have reported floods as results of very heavy rain days and very wet days (R95p), and extremely wet days (R99p) (Kilavi et al. 2018). For these locations and regions, the use of accurate forecasts for flood disaster risk reduction, preparation of response action, and most importantly proper planning of city drainage systems will reduce the vulnerability of the population

3.7 Detrended fluctuation analysis (DFA)

Table 3 presents the results for DFA for individual meteorological stations in EA. Results showed a scaling exponent 'a' for Rx1day index satisfying the condition; $0.5 < a < 1$ for most stations with exception of Garissa, Dar es Salaam, Mbeya, and Nyanza-Lac with 0.49 each. For all the stations with DFA scaling component 'a' in the range of $0.5 < a < 1$, the values of each sequence were not independent, and all exhibit long-range correlation, indicating that the future trend in each station was consistent with the change in trend over the past years analyzed (1960-2017). This implies that the Rx1day index will continue to decrease or increase at these stations as previously obtained by statistical analysis (Table 2). Perhaps, it is important to note that the Rx1day index revealed a statistically significant negative trend at Wajir and Entebbe stations in rainfall zone 1 and 6 respectively. Conversely; Rx5day indicated a scaling component fulfilling the conditions; $0.5 < a < 1$ for all the stations. The most notable scaling exponent of 0.55 is obtained at Dagoretti station which had previously shown a negative trend (Table 2); pointing that the current observed negative trend is most likely to persist at Dagoretti station than any other station. Similarly; the SDII index also indicated DFA scaling component "a" in the range of; $0.5 < a < 1$ for most stations except at Marsabit and Jinja stations. This also implies the currently observed trends at the stations will remain except for those two stations. Most importantly, the latter station had previously expressed a positive statistically significant trend for the SDII index (Table 2).

For the case of CDD and CWD indices, most stations also showed DFA scaling exponent "a" in the range of $0.5 < a < 1$. Few stations including; Narok, Namulonge, Tororo, Kiige, Kampala indicated a DFA scaling component showed that; $0 < a < 0.5$, for CDD index, while for CWD index; stations like Garissa, Wajir, Namulonge, Soroti, and Masindi showed the same trend as the latter stations, this implies the values of the sequence are not independent and therefore represent a short-range correlation or anti-persistence, which symbolizes that the data series has the opposite trend relative to that of the previous results (Table 2).

Further; for rainfall Indices; R10mm, R20mm, and R25mm, the currently observed trends are bounds to persist at most stations as indicated by DFA scaling exponent "a" which are in the range of; $0.5 < a < 1$. In the case of the R10mm index, conditions of non-future persistence are exhibited at Kiige and Kampala stations. Meanwhile; Jinja, Entebbe, and Mbarara will not experience the persistence of current trends in the R20mm Index. Likewise, only Dagoretti, Lira, Mbeya, and Kisumu stations showed no future persistence of current trends in the R25mm Index as the DFA scaling exponent of their previous trend showed the condition of opposite trend ($0 < a < 0.5$) (Table 2),

For the remaining indices that measure the rainfall depth; R95P, R99P, and PRCPTOT; results showed DFA scaling exponent "a" in the range of $0.5 < a < 1$ in nearly all stations except Kiige and Mbarara with; $0 < a < 0.5$. For R99p; the trend is similar to the R95p in which a few stations showed scaling exponent "a" in range of; $0 < a < 0.5$. These include; Dar es salaam, Dagoretti, Tororo, Soroti, and Mbeya. And a nearly equal number of stations showed scaling exponent "a" $0.5 < a < 1$ and a half other stations revealed the scaling exponent 'a' in the range of; $0 < a < 0.5$ for PRCPTOT (Table 2).

Table 3. Shows DFA scaling exponent of extreme rainfall indices for 26 stations taken at individual and as an average over 8 rainfall zones over EA. DFA scaling exponent 'a' showing; 0.5 < a < 1, implies that the current observed trend in the index (Table 2) will persist, while those DFA values in the range $0 < a < 0.5$ ***(bold in Asterik*), opposite trend relative to that of the previous time series.***

Stations	Rx1day	Rx5day	SDII	R10mm	R20mm	R25mm	CDD	CWD	R95P	R99P	PRCPTOT
Wajir	0.50	0.52	0.52	0.51	0.53	0.51	0.51	**0.47***	0.53	0.51	**0.49***
Garissa	**0.49***	0.52	0.53	0.51	0.52	0.52	0.50	**0.48***	0.52	0.55	0.52
Marsabit	0.51	0.50	**0.49***	0.51	0.51	0.53	0.52	0.55	0.51	0.51	0.51
DAR	**0.49***	0.53	0.51	0.51	0.53	0.51	0.54	0.52	0.51	**0.47***	0.52
Dagoretti	0.53	0.55	0.52	0.53	0.51	**0.49***	0.52	0.52	0.50	**0.48***	0.51
Narok	0.51	0.51	0.51	0.51	0.51	0.50	**0.49***	0.51	0.51	0.53	0.52
Namulonge	0.51	0.53	0.52	0.53	0.54	0.52	**0.49***	**0.49***	0.52	0.54	0.50
Tororo	0.50	0.52	0.54	0.51	0.60	0.54	**0.49***	0.50	0.51	**0.47***	**0.48***
Soroti	0.50	0.52	0.53	0.52	0.51	0.51	0.53	**0.49***	0.50	**0.48***	0.52
Jinja	0.52	0.52	**0.47***	0.51	**0.49***	0.53	0.51	0.51	0.53	0.52	0.55
Lira	0.51	0.51	0.50	0.51	0.50	**0.49***	0.51	0.51	0.52	0.54	0.51
Serere	0.53	0.53	0.54	0.53	**0.49***	0.50	0.52	0.53	0.52	0.54	0.51
Kiige	0.52	0.51	0.50	**0.49***	0.54	0.56	**0.49***	0.54	**0.47***	0.51	**0.48***
Mbeya	**0.49***	0.54	0.52	0.56	0.50	**0.48***	0.51	0.51	0.51	**0.47***	0.52
Bukoba	0.53	0.50	0.50	0.52	0.54	0.52	0.51	0.53	0.52	0.53	0.54
Kisumu	0.50	0.52	0.53	0.53	0.51	0.49	0.50	0.52	0.51	0.52	0.52
Kampala	0.51	0.50	0.52	**0.49***	0.50	0.52	**0.48***	0.55	0.50	0.50	**0.48***
Entebbe	0.52	0.51	0.51	0.53	**0.46***	0.52	0.50	0.51	0.50	0.52	0.55
Mbarara	0.52	0.52	0.53	0.53	**0.49***	0.51	0.54	0.51	**0.49***	0.50	0.52
Kabale	0.52	0.52	0.53	0.50	0.52	0.53	0.52	0.54	0.51	0.52	0.52
Kasese	0.54	0.51	0.51	0.51	0.50	0.54	0.53	0.51	0.51	0.52	0.51
Masindi	0.53	0.51	0.54	0.52	0.52	0.52	0.53	**0.49***	0.52	0.50	**0.49***
Gitega	0.52	0.52	0.52	0.51	0.52	0.51	0.54	0.53	0.55	0.53	**0.48***
Nyagatare	0.52	0.54	0.50	0.50	0.51	0.51	0.52	0.50	0.54	0.55	**0.49***
Nyanza lac	**0.49***	0.50	0.51	0.53	0.56	0.53	0.52	0.54	0.51	0.52	0.51
Gisenyi	0.50	0.51	0.53	0.50	0.52	0.51	0.50	0.51	0.54	0.58	0.54

3.7 Detrended fluctuation analysis (DFA) for rainfall zones (R1-R8).

To examine the changing trend in future extreme precipitation events; a long-range correlation (DFA) was performed based on key rainfall indices of significant importance. Results for r95p and r99p indices for the 8 rainfall zones of EA are presented in (Fig.3). The result showed that the DFA scaling exponent 'a' in r95p and r99p indices varied from one region to the other. For r95p index, the results for 8 regions (R1-R8) were; 0.46, 0.515, 0.53, 0.518, 0.512, 0.517, 0.0504, and 0.524 respectively. In this case, with exception of R1, the remaining sequence was not independent, and all exhibit long-range correlation, indicating that the future trend in each region is consistent with the change in trend over the past years analyzed. This implies that r95p will continue to decrease or increase in the regions as previously obtained by statistical analysis (Table 2).

Similarly; for the r99p index for all rainfall zones (R1-R8) shown in the lower parts of Fig. 3, the DFA scaling exponent 'a' were; 0.519, 0.53, 0.49, 0.48, 0.54; 0.517, 0.513, and 0.528 respectively. Like in the case of r95p, all the regions with the scaling factor 'a' $\geq$5 will continue to decrease or increase as previously obtained for the past years (1960-2017) by statistical analysis of trend presented in Table 2.

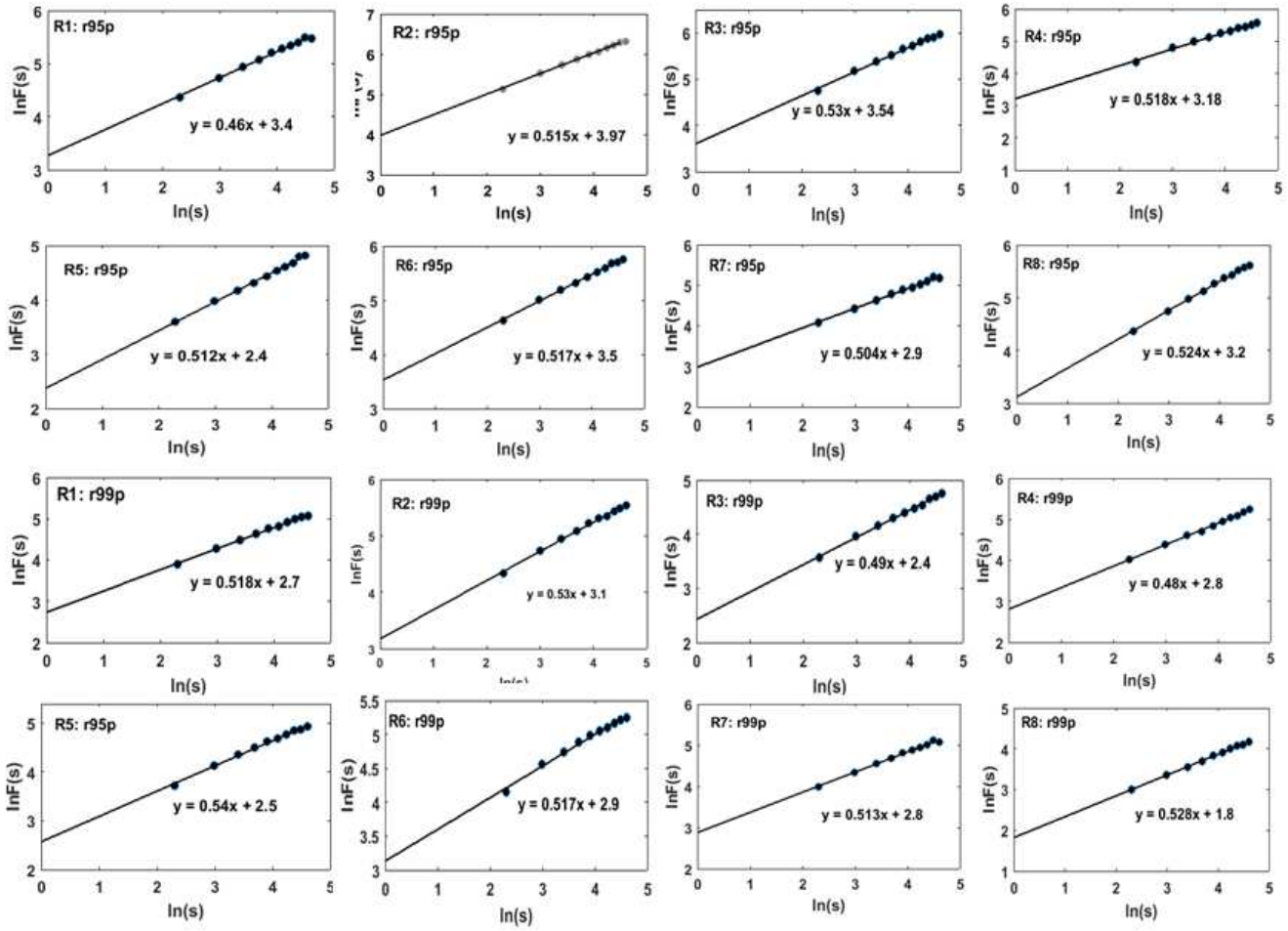

Fig.3. Shows Detrended Fluctuation Analysis (DFA) for long-range forecasting of extreme precipitation indices (r95p) and r99p for 8 rainfall zones (R1-R8) over East Africa.

In other related precipitation Indices such as CDD and CWD (Fig 4); DFA scaling exponent was able to reveal consistent results in some regions while others were not consistent. For example; scaling component 'a' for CDD shown on the upper part of Fig.4 for rainfall zones (R1-R8) were; 0.517, 0.53, 0.48, 0.48, 0.55, 0.46, 0.49, and 0.511 respectively. The results show that half of the region (R1, R2, R5, and R8), had a DFA scaling component 'a' is greater than 0.5 or $0.5 < a < 1$, the values of each of this sequence were therefore not independent, and all these regions had a long-range correlation with previous years, meaning that the future trend in CDD index was consistent with the change in trend over the past years analyzed (19650–2017). This implies that CDD will continue to decrease or increase in the regions as previously obtained by statistical analysis of historical CDD over EA as shown in Table 2.

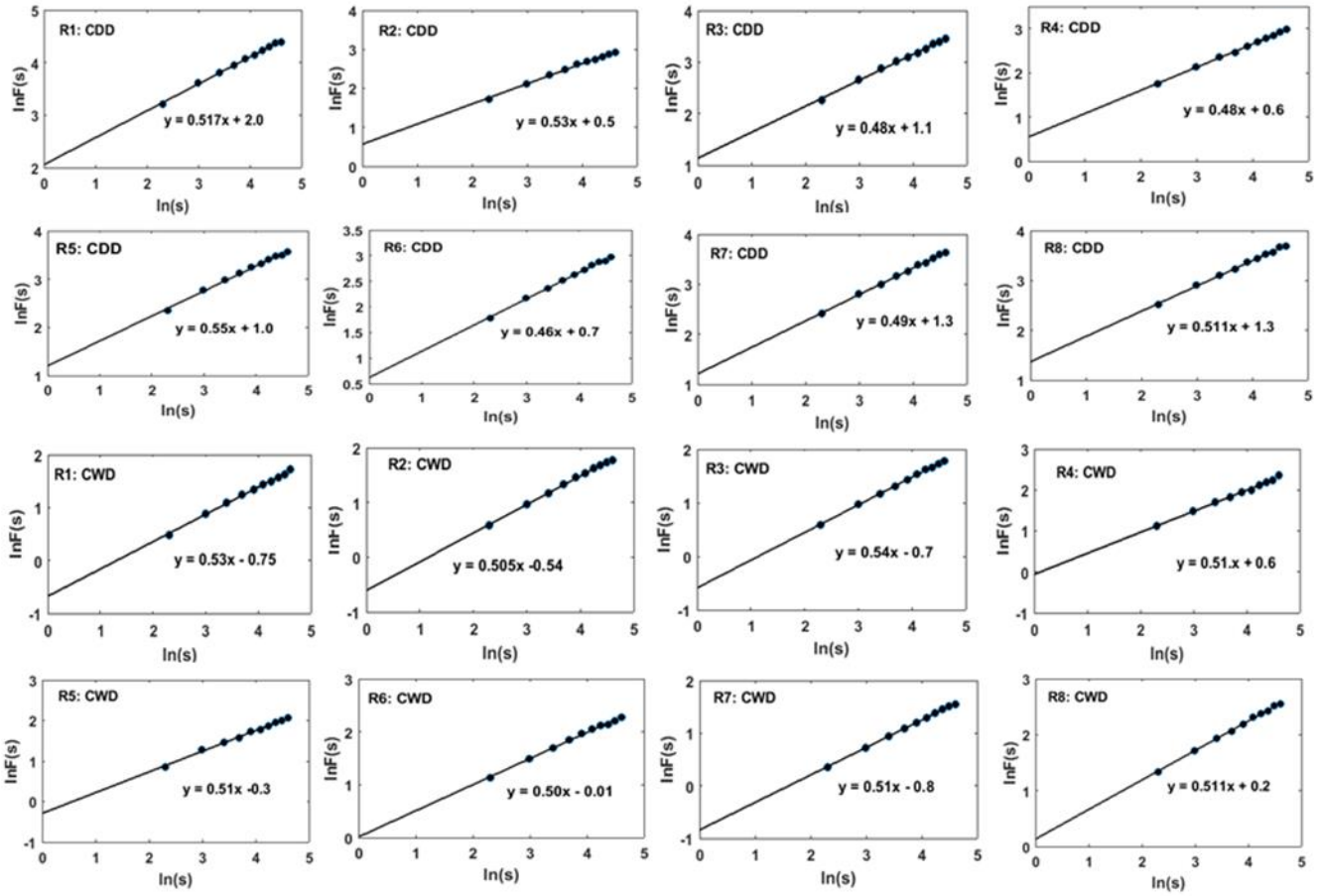

Fig.4. Detrended Fluctuation Analysis (DFA) for long-range forecasting of extreme precipitation indices CDD and CWD for 8 rainfall zones (R1-R over East Africa

The results for R10mm and R20mm rainfall indices presented in upper Fig.5 also show varied DFA scaling component 'a' in both Indices. For example; for R10 index, the factors were; 0.513, 0.53, 0.502, 0.55, 0.506, 0.51, 0.50, and 0.51 respectively. All regions, therefore, show that the values of each sequence were therefore not independent, and all had long-range correlation, meaning that the future trend in the DFA index was consistent with the change in trend over the past years analyzed (1960–2017). This implies that R10mm will continue to decrease or increase in the regions as previously obtained by statistical analysis of historical of DFA over EA.

The results for R20mm rainfall indices presented in the lower part of (Fig.5) also show varied DFA scaling component 'a' in different regions. The scaling component 'a' were; 0.514, 0.512, 0.520, 0.500, 0.53, 0.52, 0.47, and 0.49 respectively. The first 6 regions (R1-R6), therefore, show that the values of each sequence were therefore not independent, and all had long-range correlation, meaning that the future trend in the DFA index was consistent with the change in trend over the past years analyzed (19650–

2017). This implies that R20mm will continue to decrease or increase in the regions as previously obtained by statistical analysis of the historical trends over EA as presented in Table 2.

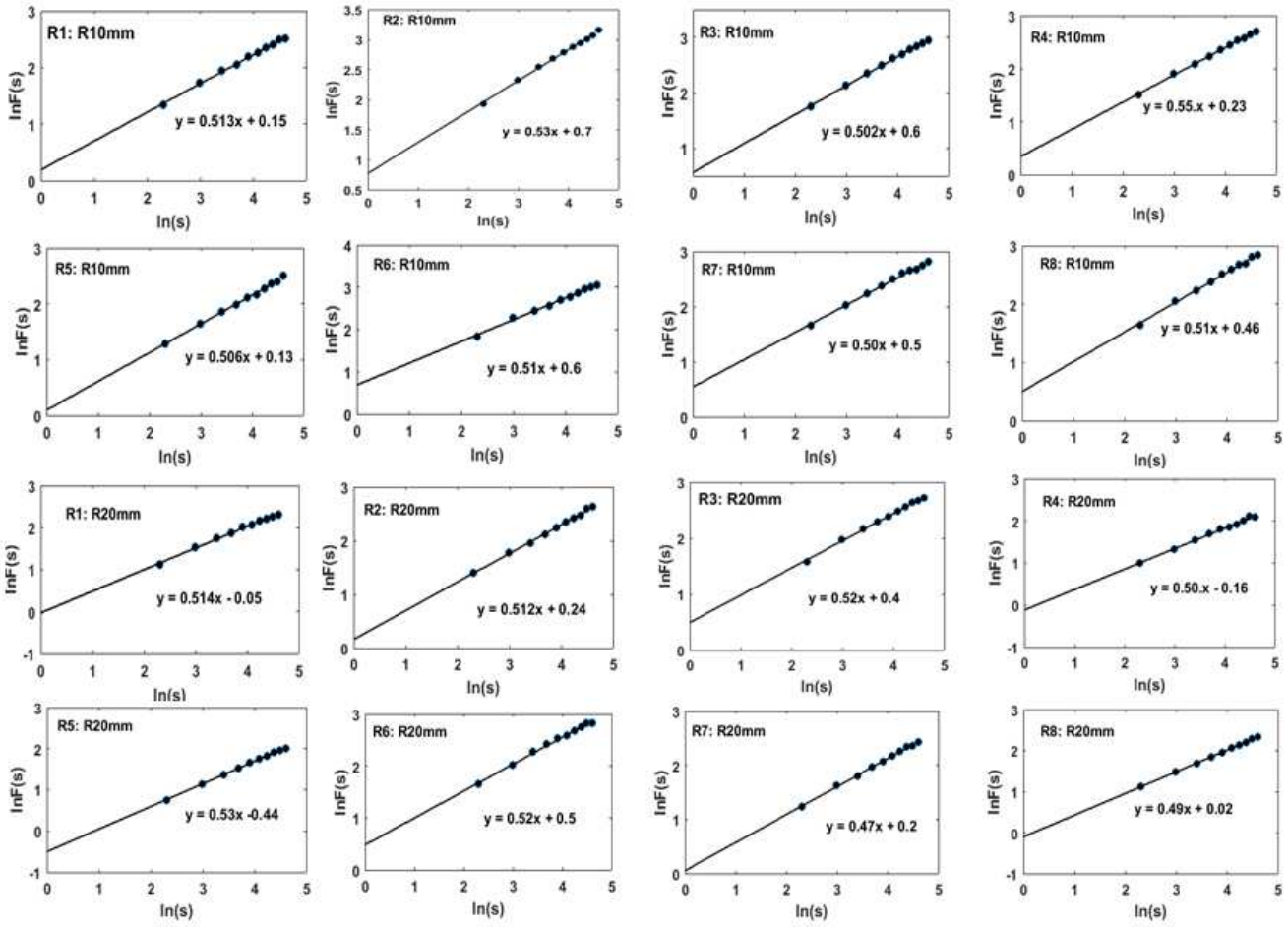

Fig.5. Detrended Fluctuation Analysis (DFA) for long-range forecasting of extreme precipitation indices R10mm and R20mm for 8 rainfall zone (R1-R) over East Africa.

The results for RX1day indices presented in the upper part of (Fig.6) also show varied DFA scaling component 'a' for the period analyzed. The scaling component 'a' were; 0.52, 0.52, 0.51, 0.500, 0.53, 0.52, 0.50, and 0.48 respectively. The first 7 regions (R1-R7) regions, therefore, show that the values of each sequence were therefore not independent, and all had long-range correlation, meaning that the future trend in the DFA index was consistent with the change in trend over the past years analyzed (19650–2017). This implies that RX1day will continue to decrease or increase in the regions as previously obtained by statistical analysis of historical of DFA over EA (see Table 2).

The results for RX5day indices presented in the lower part of (Fig.6) also show varied DFA scaling component 'a' for the period analyzed. The scaling component 'a' were; 0.52, 0.52, 0.52, 0.46, 0.52, 0.48, 0.53, and 0.51 respectively. With exception of R4 and R7, the remaining region (R1-R3, R5, and R8)

regions, therefore, show that the values of each sequence were therefore not independent, and all had a long-range correlation, meaning that the future trend in the DFA index was consistent with the change in trend over the past years analyzed (1960–2017). This implies that RX5day will continue to decrease or increase in the regions as previously obtained by statistical analysis of historical DFA over EA.

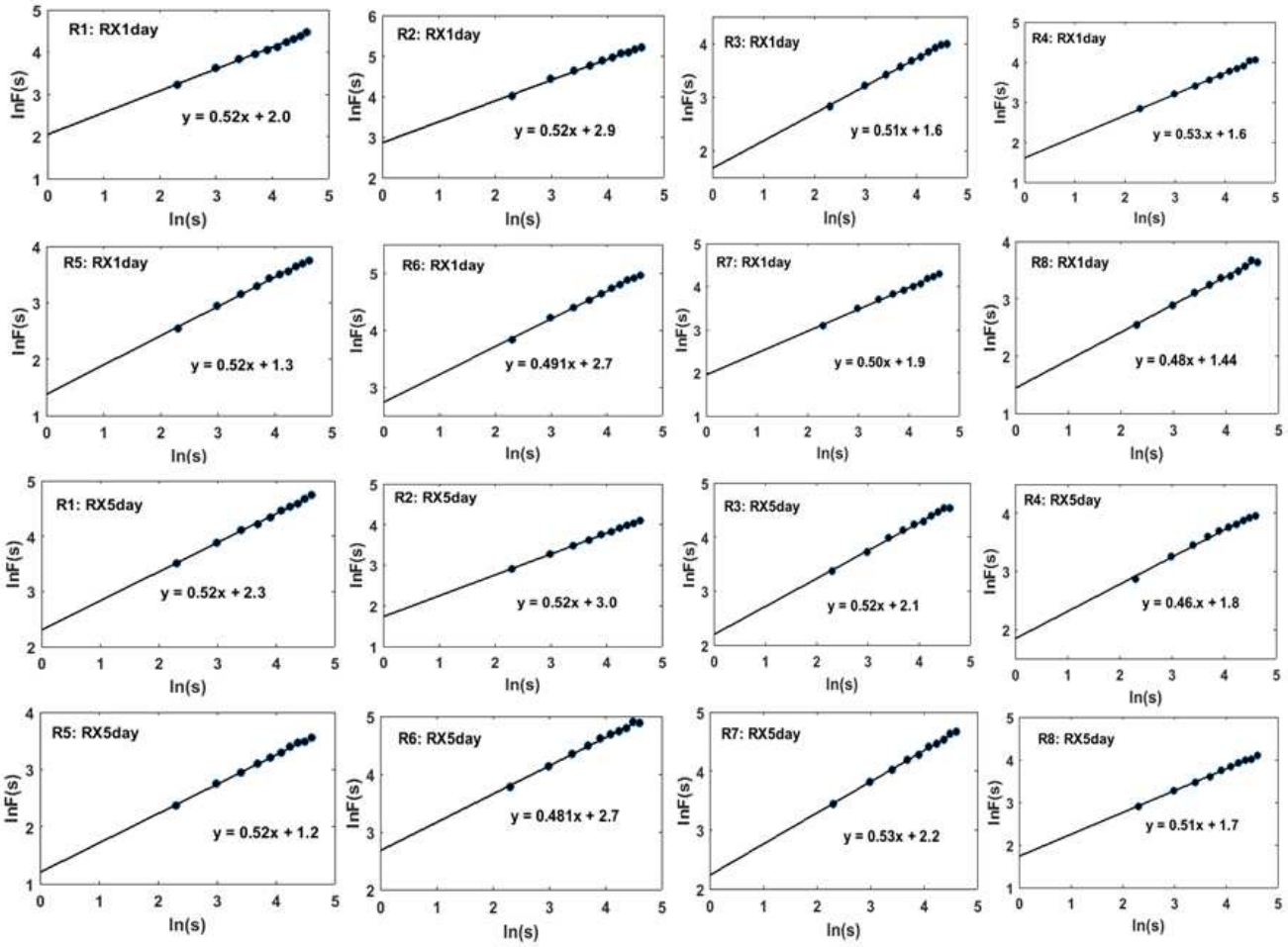

Fig.6. Detrended Fluctuation Analysis (DFA) curves for long-range forecasting of extreme precipitation indices RX1day and RX5 days for 8 rainfall zone (R1-R) over East Africa

Figure.7. Shows the correlation coefficient diagram between rainfall extreme indices and the atmospheric teleconnections indices (DMI and Nino 3.4) over EA. Results showed a low correlation of extreme rainfall events in the regions; i.e there is no close relationship between an extreme event occurring in one region to the other. For instance, for PRCPTOT, the best correlation coefficient (0.47) is shown between rainfall zone 3 (R3) and rainfall Zone 1(R1), followed by 0.41 between R1 and R5. The existence of a low correlation coefficient of extreme events between rainfall zones (R1-R8) is common in

all rainfall extreme events. This implies that the development of appropriate adaptation and mitigation strategies should be done location-specific as there are low chances of regions experiencing similar extreme events.

3.8 Zonal variability of extreme rainfall events and the relationship ENSO and IOD

Figure 7 shows the correlation coefficient diagram between rainfall extreme indices and the atmospheric teleconnections indices (DMI and Nino 3.4) over eight rainfall zones (R1-R8) in EA. Results showed a low correlation of extreme rainfall events in the regions; i.e there is no close relationship between extreme events occurring in one region to the other. For instance, for PRCPTOT, the best correlation coefficient (0.47) is shown between rainfall zone 3 (R3) and rainfall Zone 1(R1), followed by 0.41 between R1 and R5. The existence of a low correlation coefficient of extreme events between rainfall zones (R1-R8) is common in all the rainfall extreme events (Fig.7). This implies that the development of appropriate adaptation and mitigation strategies should be done location-specific as there are low chances of regions experiencing similar extreme events due to inhomogeneity of rainfall events.

Regarding the relationship between extreme indices and the two atmospheric teleconnections, results showed both negative and positive correlations in the rainfall zones (Table 4). For instance, most rainfall zones showed a positive correlation between PRCPTOT and IOD (Dipole Mode Index-DMI) except R2, while an equal number of positive and negative correlations revealed between ENSO-(Nino 3.4) and the same Index in the rainfall zones. The highest correlation (r =0.35) is between DMI and PRCPTOT index in rainfall zone 7(R7). Similarly, most rainfall zones showed a positive correlation between the R95p index and DM, while 5 out of 8 rainfall zones experienced a negative correlation between ENSO-Nino 3.4 index and R95p, with r=0.33 as the highest correlation still obtained in R7. For all remaining indices, R20mm, RX5day, CDD, and CWD, similar trends are observed where a more positive correlation is revealed between DMI and negative results with ENSO-Nino 3.4 Index.

Table 4: Show a summary of the correlation coefficient (r) of different extreme rainfall index and two atmospheric teleconnections (DMI and Nino 3.4) in the eight rainfall zones (R1-R8) in EA

RF	PRCPTOT		r95p		R20 mm		RX5day		CDD		CWD	
Zone	DMI	Nino3.4	DMI	Nino3.4	DMI	Nino3.4	DMI	Nino3.4	DMI	Nino3.4	DMI	Nino3.4
R1	0.17	0.05	0.31	-0.07	0.19	-0.01	0.31	-0.03	-0.05	-0.07	0.23	-0.04
R2	-0.02	-0.06	0.24	0.07	0.20	0.09	-0.09	0.17	-0.15	-0.05	-0.05	0.23
R3	0.18	0.18	0.34	0.21	0.29	0.22	0.26	0.07	0.31	-0.03	-0.07	-0.09
R4	0.12	0.05	0.22	-0.07	0.26	-0.02	0.04	0.22	0.07	-0.06	0.11	0.00
R5	0.14	-0.04	-0.02	-0.01	0.20	-0.06	-0.18	-0.11	-0.04	0.23	-0.23	-0.21
R6	0.17	-0.01	0.03	-0.06	-0.02	-0.10	0.02	-0.07	-0.04	0.25	0.21	-0.01
R7	0.35	0.09	0.33	-0.01	0.14	0.04	0.17	-0.06	-0.10	0.01	0.00	-0.15
R8	0.12	-0.11	0.09	0.02	0.16	0.19	0.24	0.13	0.03	0.38	0.25	-0.11

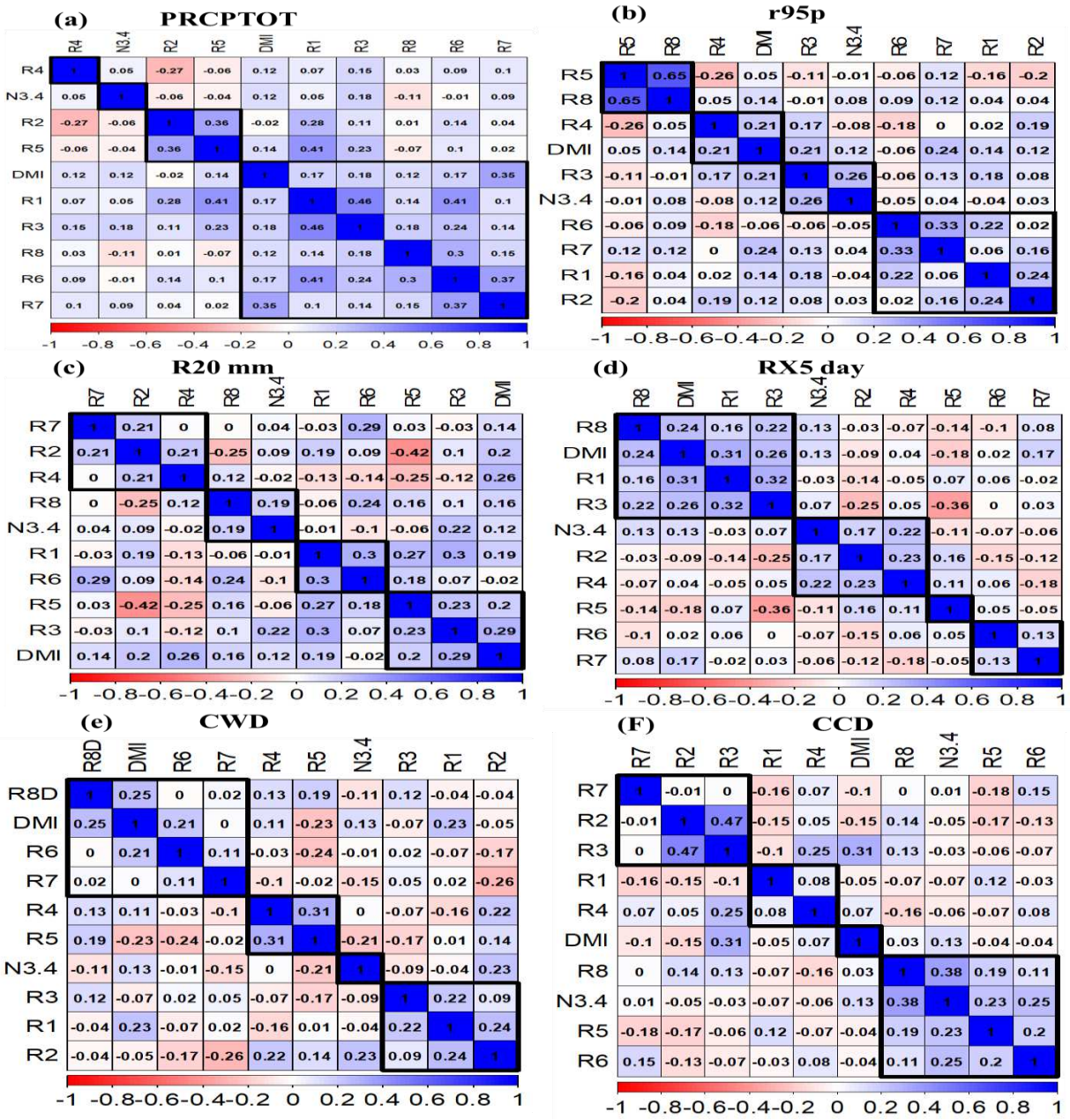

585

586

587 ***Fig. 7 shows the correlations plots for annual total wet-day precipitation (PRCPTOT) (a), very heavy rainfall***
588 ***(r95p) (b), annual count of days when precipitation≥ 20mm(c), max 5-day precipitation amount (RX5day) (d),***
589 ***consecutive wet days (CWD) (e), consecutive dry days (CCD)(f). (Note DMI= Dipole Mode Index and N3.4 =***
590 ***Nino 3.4 index).***

591

592

593

594

4.0 Conclusions

This study examined changes in the occurrence of extreme rainfall events using long-term observed rainfall records for 25 stations varying from 1960-2017. The spatial distribution of extreme rainfall events was generated by geographical information System (GIS) through the Krigging Interpolation technique. Future development of extreme rainfall events was computed using Detrended Fluctuation Analysis (DFA). Results revealed that the consecutive wet day's index (CWD) was a decreasing trend in 72% of the stations analyzed. Moreover, the consecutive dry days (CDD) index also indicated a positive trend in 44% of the stations analyzed especially in the Arid and Semi-Arid region (ASAL) of Kenya in R1.

Additionally, heavy rainfall days (R10mm) show a positive trend at 52% of the stations but the trend is statistically significant at only 3 stations; Jinja, Kisumu, and Kasese stations. The remaining 48% stations portrayed an insignificance negative trend for the R10mm index. Moreover; all the 60% (15/25) of the stations analyzed revealed a positive trend for very heavy rainfall days (R20mm) index did not present any statistical significance in the study area, for the remaining stations 40%, a statistically significant negative trend in the R20mm index, were revealed at Entebbe and Kampala. In light of the extremely heavy rainfall days (R25mm) index, 56% of the stations revealed a decreasing trend for the index where stations such as Kisumu, Entebbe in rainfall zone 6 and Gitega in rainfall zone 8 showed a statistically significant trend with a rate of decrease of -0.164 mm/year, -0.129 mm/year, and -0.157 mm/year respectively. It can be observed that there is an increasing tendency in all two indices that relates to heavy rainfall days (R10mm), and very heavy rainfall days (R20mm) which are associated to flash floods. Statistically insignificant negative and positive trends are also revealed for the very wet day's index (R95p), and extremely wet days index (R99p), and the most important results have been noticed in rainfall zone 4 where numerous floods and drought events are reported in the area.

Results showed a low correlation coefficient of extreme rainfall events in the regions; i.e there is no strong relationship between extreme events occurring in one region to the other. Similarly, the correlation coefficient between rainfall extreme indices and the atmospheric teleconnections indices (DMI and Nino 3.4) were generally low. For instance, most rainfall zones showed a positive correlation between PRCPTOT and IOD (Dipole Mode Index-DMI) except R2, while an equal number of positive and negative correlations revealed between ENSO-(Nino 3.4) and the same Index in the rainfall zones. The highest correlation ($r = 0.35$) is between DMI and PRCPTOT index in rainfall zone 7(R7). Similarly, most rainfall zones showed a positive correlation between the R95p index and DM, while 5 out of 8 rainfall zones experienced a negative correlation between ENSO-Nino 3.4 index and R95p, with $r = 0.33$ as the

highest correlation still obtained in R7. The impacts of highly variable trends of extremes events correspond to highly variable rainfall reported in EA which usually impacts adversely on the livelihood of the communities. DFA showed varied results, however most of the stations that the current trends is most likely to persist.

Based on these diverse results, we recommend that the development of appropriate adaptation and mitigation strategies be done location-wise as there are low chances of regions experiencing similar extreme events due to heterogeneity of rainfall events. The study provides some important information required for planning mitigation and adaptation strategies, especially in disaster preparedness. Future studies on the influence of atmospheric teleconnections on extreme events may include other variables such as North Atlantic Oscillation (NAO) index, and several high-pressure systems (e.g Mascarene, St. Hellena, Azores and Arabian Ridge, etc.) whose influence is not well known especially under the current changing climate.

Conflict of Interest

There is no conflict of interest in this paper.

Acknowledgments

The first and second authors also wish to acknowledge the support from the Chinese Scholarship Council (CSC), the National Natural Science Foundation of China (41875177; 41375159), and Nanjing University of information science and technology. The Authors of this work acknowledge the contributions of the previous Authors cited in this paper. The authors would like to acknowledge all institutions for providing precipitation data used for analysis.

Reference

Adhikari, U., Nejadhashemi, A.P., Woznicki, S.A., 2015. Climate change and eastern Africa : a review of impact on major crops. Food Energy Secur. 4, 110–132. https://doi.org/10.1002/fes3.61

Aguilar, E., Auer, I., Brunet, M., Peterson, T.C., Wieringa, J., 2003. Guidelines on Climate Metadata and Homogenization, WMO/TD No. 1186. World Meteorological Organisation, Geneva., World Meteorological Organization.

Alexander, L. V., Zhang, X., Peterson, T.C., Caesar, J., Gleason, B., Klein Tank, A.M.G., Haylock, M., Collins, D., Trewin, B., Rahimzadeh, F., Tagipour, A., Rupa Kumar, K., Revadekar, J., Griffiths, G., Vincent, L., Stephenson, D.B., Burn, J., Aguilar, E., Brunet, M., Taylor, M., New, M., Zhai, P., Rusticucci, M., Vazquez-Aguirre, J.L., 2006. Global observed changes in daily climate extremes of temperature and precipitation. J. Geophys. Res. Atmos. 111, 1–22. https://doi.org/10.1029/2005JD006290

Ayugi, B.O., Tan, G., Ongoma, V., Mafuru, K.B., 2018. Circulations Associated with Variations in Boreal Spring Rainfall over Kenya. Earth Syst. Environ. 2, 421–434. https://doi.org/10.1007/s41748-018-0074-6

Barasa, B., Vincent, K., Frank, M., 2015. International Journal of Environmental Comparison of extreme weather events and streamflow from drought indices and a hydrological model in River Malaba, Eastern Uganda. Int. J. Environ. Stud. 70, 932–943. https://doi.org/10.1080/00207233.2013.862463

Behera, S.K., Luo, J.J., Masson, S., Delecluse, P., Gualdi, S., Navarra, A., Yamagata, T., 2005. Paramount impact of the Indian Ocean dipole on the East African short rains: A CGCM study. J. Clim. 18, 4514–4530. https://doi.org/10.1175/JCLI9018.1

Bouagila, B., Sushama, L., 2013. On the Current and Future Dry Spell Characteristics over Africa. Atmosphere 4: 272–298. https://doi.org/10.3390/atmos4030272

Costa, A.C., Soares, A., 2009. Homogenization of climate data: Review and new perspectives using geostatistics. Math. Geosci. 41, 291–305. https://doi.org/10.1007/s11004-008-9203-3

Davis, R., Gichere, S., Mogaka, H., Hirji, R., 2009. Climate Variability and Water Resources in Kenya: The Economic Cost of inadequate Management; Water P-Notes, No. 22; World Bank: Washington, DC, USA, 4p.

682 Drago, A.F., Boxall, S.R., 2002. Use of the wavelet transform on hydro-meteorological data. Phys. Chem.
683 Earth 27, 1387–1399. https://doi.org/10.1016/S1474-7065(02)00076-1

684 FAO, 2017. The future of food and agriculture: Trends and challenges, Food and Agriculture
685 Organization of the United Nations.Rome, Italy.

686 Kilavi, M., MacLeod, D., Ambani, M., Robbins, J., Dankers, R., Graham, R., Helen, T., Salih, A.A.M.,
687 Todd, M.C., 2018. Extreme rainfall and flooding over Central Kenya Including Nairobi City during
688 the long-rains season 2018: Causes, predictability, and potential for early warning and actions.
689 Atmosphere (Basel). 9. https://doi.org/10.3390/atmos9120472

690 Fraedrich, K., Blender, R., 2003. Scaling of Atmosphere and Ocean Temperature Correlations in
691 Observations and Climate Models. Phys. Rev. Lett. 90, 4.
692 https://doi.org/10.1103/PhysRevLett.90.10850

693 Gamoyo, M., Reason, C., Obura, D, 2015. Rainfall variability over the East African coast. Theor Appl
694 Climatol 120:311–322. https://doi.org/10.1007/s00704-014-1171-6

695 Gebrechorkos, S.H., Hülsmann, S., Bernhofer, C., 2019. Long-term trends in rainfall and temperature
696 using high-resolution climate datasets in East Africa. Sci. Rep. 9, 1–9.
697 https://doi.org/10.1038/s41598-019-47933-8

698 Gitau, W., Camberlin, P., Ogallo, L., Bosire, E., 2018. Trends of intraseasonal descriptors of wet and dry
699 spells over. Int. J. Climatol. 38, 1189–1200. https://doi.org/10.1002/joc.5234

700 Hague, T., 2010. Projected Changes in Mean and Extreme Precipitation in Africa under Global Warming.
701 Part II : East Africa 3718–3733. https://doi.org/10.1175/2010JCLI2883.1

702 Indeje, M., Semazzi, F.H.M., Ogallo, L.J., 2000. ENSO Signals in East African rainfall seasons. Int. J.
703 Climatol. 46, 19–46. https://doi.org/10.1002/(SICI)1097-0088(200001)20:1<19::AID-
704 JOC449>3.0.CO;2-0

705 Kansiime, M.K., Wambugu, S.K., Shisanya, C.A., 2013. Perceived and Actual Rainfall Trends and
706 Variability in Eastern Uganda : Implications for Community Preparedness and Response. J. Nat. Sci.
707 Res. 3, 179–195.

708 Kilavi, M., MacLeod, D., Ambani, M., Robbins, J., Dankers, R., Graham, R., Helen, T., Salih, A.A.M.,

709 Todd, M.C., 2018. Extreme rainfall and flooding over Central Kenya Including Nairobi City during
710 the long-rains season 2018: Causes, predictability, and potential for early warning and actions.
711 Atmosphere (Basel). 9. https://doi.org/10.3390/atmos9120472

712 Kizza, M., Rodhe, A., Xu, C.-Y., Ntale, H.K., Halldin, S., 2009. Temporal rainfall variability in the Lake
713 Victoria Basin in East Africa during the twentieth century. Theor. Appl. Climatol. 98, 119–135.
714 https://doi.org/10.1007/s00704-008-0093-6

715 Kiros, G., Shetty, A., Nandagiri, L., 2017. Extreme rainfall signatures under changing climate in semi-
716 arid northern highlands of Ethiopia. Cogent Geosci. 3, 1–20.
717 https://doi.org/10.1080/23312041.2017.1353719

718 Lyon, B., Dewitt, D.G., 2012. A recent and abrupt decline in the East African long rains 39, 1–5.
719 https://doi.org/10.1029/2011GL050337

720 Mubiru, D.N.; Komutunga, Everline; Agona, Ambrose; Apok, Anne; Ngara, T., 2012. Characterising
721 agrometeorological climate risks and uncertainties : Crop production in Uganda. S. Afr. J. Sci.
722 108(3–4), 108–118. https://doi.org/10.4102/sajs.v108i3/4.470

723 Mumo, L., Yu, J., Ayugi, B.O., 2019. Evaluation of spatiotemporal variability of rainfall over Kenya from
724 1979 to 2017. J. Atmos. Solar-Terrestrial Phys. 194, 105097.
725 https://doi.org/10.1016/j.jastp.2019.105097

726 Nicholson, S.E., 2017. Climate and climatic variability of rainfall over eastern Africa. Rev. Geophys. 55,
727 590–635. https://doi.org/10.1002/2016RG000544

728 Nimusiima, A., Basalirwa, C.P.K., Majaliwa, J.G.M., Otim-Nape, W., Okello-Onen, J., Rubaire-Akiiki,
729 C., Konde-Lule, J..Ogwal-Byenek, S., 2013. Nature and dynamics of climate variability in the
730 Uganda cattle corridor. African J. Environ. Sci. Technol. 7, 770–782.
731 https://doi.org/10.5897/AJEST2013.1435

732 Nkunzimana, A., Bi, S., Jiang, T., Wu, W., Abro, M.I., 2019. Spatiotemporal variation of rainfall and
733 occurrence of extreme events over Burundi during 1960 to 2010. Arab. J. Geosci. 12, 0–22.
734 https://doi.org/10.1007/s12517-019-4335-y

735 Ogwang, B.A., Chen, H., Tan, G., Ongoma, V., Ntwali, D., 2015a. Diagnosis of East African climate and
736 the circulation mechanisms associated with extreme wet and dry events: A study based on RegCM4.

737 Arab. J. Geosci. 8, 10255–10265. https://doi.org/10.1007/s12517-015-1949-6

738 Ogwang, B.A., Ongoma, V., Gitau, W., 2016. Contributions of atlantic ocean to June-August rainfall over
739 Uganda and Western Kenya. J. Earth Sp. Phys. 41, 131–140.

740 Ogwang, B.A., Ongoma, V., Xing, L., Ogou, F.K., 2015b. Influence of Mascarene high and Indian Ocean
741 dipole on East African extreme weather events. Geogr. Pannonica 19, 64–72.
742 https://doi.org/10.18421/GP19.02-05

743 Ojara, M.A., Lou, Y., Aribo, L., Namumbya, S., Uddin, M.J., 2020. Dry spells and probability of rainfall
744 occurrence for Lake Kyoga Basin in Uganda, East Africa. Nat. Hazards 100, 493–514.
745 https://doi.org/10.1007/s11069-019-03822-x

746 Omondi, P.A., Awange, J.L., Forootan, E., Ogallo, L.A., Barakiza, R., Girmaw, G.B., Fesseha, I.,
747 Kululetera, V., Kilembe, C., Mbati, M.M.M., Kilavi, M., King'uyu, S.M., Omeny, P.A., Njogu, A.,
748 Badr, E.M., Musa, T.A., Muchiri, P., Bamanya, D., Komutunga, E., Aming, P., Awange, J.L.,
749 Forootan, E., Ogallo, A., Girmaw, B., Fesseha, I., Kululetera, V., Mbati, M.M.M., Kilavi, M., King,
750 M., Adek, P., Njogu, A., Badr, M., Musa, A., Muchiri, P., Komutunga, E., 2013. Changes in
751 temperature and precipitation extremes over the Greater Horn of Africa region from 1961 to 2010.
752 Int. J. Climatol. 34, 1262–1277. https://doi.org/10.1002/joc.3763

753 Ongoma, V., Chen, H., Gao, C., Chena, H., Gaoa, C., 2017. Projected changes in mean rainfall and
754 temperature over East Africa based on CMIP5 models. Int. J. Climatol. 38, 1375–1392.
755 https://doi.org/10.1002/joc.5252

756 Ongoma Victor, Haishan Chen, G.W.O., 2018. Variability of extreme weather events over the equatorial
757 East Africa, a case study of rainfall in Kenya and Uganda. Theorectical Appl Climatol. 295–308.
758 https://doi.org/10.1007/s00704-016-1973-9

759 Onyutha, C., 2016. Geospatial trends and decadal anomalies in extreme rainfall over Uganda, East Africa.
760 Adv. Meteorol. 2016. https://doi.org/10.1155/2016/6935912

761 Owor, M., Taylor, R.G., Tindimugaya, C., Mwesigwa, D., 2009. Rainfall intensity and groundwater
762 recharge : empirical evidence from the. Environ. Res. Lett. 4(3):035009
763 https://doi.org/10.1088/1748-9326/4/3/035009

764 Peng, C.K., Buldyrev, S.V., Havlin, S., Simons, M., Stanley, H.E., Goldberger, A.L., 1994. Mosaic

765 organization of DNA nucleotides. Phys. Rev. E 49 (2), 1685–1689

766 Schlenker, W., Lobell, D.B., 2010. Robust negative impacts of climate change. Environ. Res. Lett. 5.
767 014010 (8pp). https://doi.org/10.1088/1748-9326/5/1/014010

768 Sillmann, J., Kharin, V. V., Zhang, X., Zwiers, F.W., Bronaugh, D., 2013. Climate extremes indices in the
769 CMIP5 multimodel ensemble: Part 1. Model evaluation in the present climate. J. Geophys. Res.
770 Atmos. 118, 1716–1733. https://doi.org/10.1002/jgrd.50203

771 Rowell, D., Booth, B., Nicholson.S, Good, P., 2015. Reconciling Past and Future Rainfall Trends over
772 East Africa. J. Clim. 28: 9768–9788. https://doi.org/10.1175/JCLI-D-15-0140.1

773 Takaoka, S., 2005. Impact of the 1997 – 1998 El Niño Rains on Farms in the Mount Kenya Region. Int.
774 Mt. Soc. 25, 326–331. https://doi.org/doi.org/10.1659/0276-4741(2005)025[0326:IOTENR]2.0.CO;2

775 Tilya, F.F., Mhita, M.S.,2007 Frequency of Wet and Dry Spells in Tanzania. In: Sivakumar MVK,
776 Ndiang'ui N. (eds) Climate and Land Degradation. Environmental Science and Engineering
777 (Environmental Science). Springer, Berlin, Heidelberg. p197-204. https://doi.org/10.1007/978-3-
778 540-72438-4_10

779 Tong, S., Li, X., Zhang, J., Bao, Yuhai, Bao, Yongbin, Na, L., Si, A., 2019. Spatial and temporal
780 variability in extreme temperature and precipitation events in Inner Mongolia (China) during 1960–
781 2017. Sci. Total Environ. 649, 75–89. https://doi.org/10.1016/j.scitotenv.2018.08.262

782 Tsinda, A, Kind, C, H.J.., 2014. Estimating damage costs of flooding on small- and medium-sized
783 enterprises in Kigali, Rwanda. J. Disaster Risk Stud. 11, 1–11.

784 Varotsos, C.A., Ondov, J.M., Cracknell, A.P., Efstathiou, M.N., Assimakopoulos, M.N., 2006. Long-
785 range persistence in global Aerosol Index dynamics. Int. J. Remote Sens. 27, 3593–3603.
786 https://doi.org/10.1080/01431160600617236

787 WMO, 2013. Guide to climatological practices (3rd edition). World Meteorological Organization
788 (WMO), Geneva

789 Yang, W., Seage, R., Cane, M.A., Lyon, B., 2014. The East African Long Rains in Observations and
790 Models. J. Clim. 7185–7202. https://doi.org/10.1175/JCLI-D-13-00447.1

791 Zhang, X., Alexander, L., Hegerl, G.C., Jones, P., Tank, A.K., Peterson, T.C., Trewin, B., Zwiers, F.W.,

2011. Indices for monitoring changes in extremes based on daily temperature and precipitation data 2. https://doi.org/10.1002/wcc.147

794 **Table S1: Shows the codes, indicator names,5`8 and descriptions of 11 rainfall indices**

Code	Indicator name	Description of Indicator	Units
SDII	Simple Daily Intensity Index	Mean precipitation amount that is registered on wet days	mm
Rx1day	Max 1-day precipitation amount	Maximum 1-day precipitation total	mm
Rx5day	Max 5-day precipitation amount	Maximum 5-day precipitation total	mm
CDD	Consecutive dry days	Maximum number of consecutive days with RR<1 mm	Days
R10 mm	Annual count of days	Number of days with more than 10 mm of precipitation days	Days
R20mm	Annual count of days	Annual count of days when PRCP≥ 20mm	Days
R25mm	Annual count of days	Annual count of days when PRCP≥ 25mm	Days
CWD	Consecutive wet days	Maximum number of consecutive days with RR >=1 mm	Days
R95p	Very wet days	Annual total PRCP when RR>95th percentile	mm
R99p	Extremely wet days	Annual total PRCP when RR > 99th percentile	mm
PRCPTOT	Annual total wet-day precipitation	Annual total PRCP in wet days (RR >=1 mm)	mm

795

796

797

798

799

Table S2. Shows the statistical metrics for evaluation of the performance of satellite datasets(CHIRPS), over 8 rainfall zones of EA(R1-R8). (R= correlation coefficient, RMSD is the root mean squared difference, BIAS is the statistical bias)

Rainfall	R	RMSD	BIAS
R1	0.92	24.93	-1.32
R2	0.9	39.41	-14.18
R3	0.91	22.99	0.42
R4	0.83	36.77	-16.46
R5	0.94	32.02	17.03
R6	0.9	31.4	-18.33
R7	0.83	30.24	-3.86
8	0.95	21.37	-0.29

Table S2 Shows preliminary quality control result for rainfall datasets for 25 station. The p-values for the Shapiro-Wilk normality test (htest), Grubbs outlier test (qgrubbs), Standard Normal Homogeneity Test (SNHT), and Buishand range test (BR)

Station	**Longitude**	**Latitude**	**Elevation**	**Period**	**"htest**	**qgrubbs**	**SNHT**	**BR**
Wajir	41.9	3.9	271	1960-2016	0.085	0.072	0.233	0.464
Garissa	40.1	1.8	246	1957-2016	0.084	0.074	0.135	0.387
Marsabit	38.02	2.31	1283	1960-2016	0.9	0.054	0.139	0.257
DAR	39.12	-6.8	156	1960-2017	0.941	0.278	0.15	0.282
Dagoretti	36.75	-1.31	1830	1961-2016	0.109	0.291	0.193	0.124
Narok	35.91	-1.1	1950	1964-2016	0.285	0.43	0.247	0.513
Namulonge	32.6	0.51	1128.1	1963-2017	0.893	0.149	0.163	0.073
Tororo	34.21	0.71	1176.2	1970-2017	0.096	0.128	0.243	0.12
Soroti	33.6	1.7	1115	1961-2017	0.059	0.03	0.228	0.173
Jinja	33.11	0.51	1175	1961-2017	0.571	0.092	0.122	0.061
Lira	32.9	2.32	1120.4	1971-2017	0.317	0.242	0.173	0.083
Serere	33.5	1.5	1098.2	1961-2017	0.07	0.232	0.169	0.209
Kiige	33	1.1	1089.1	1971-2017	0.07	0.054	0.11	0.405
Bukoba	31.82	-3.37	1144	1960-2017	0.609	0.981	0.137	0.081
Mbeya	33.47	-8.93	1791	1980-2017	0.083	0.924	0.066	0.335
Kisumu	34.8	-0.1	1154	1980-2016	0.866	0.129	0.26	0.278
Kampala	32.62	0.32	1162	1980-2016	0.893	0.149	0.163	0.203
Entebbe	32.62	0.53	1117	1951-2016	0.423	0.134	0.085	0.12
Mbarara	30.41	-0.13	1408	1950-2016	0.052	0.09	0.583	0.143
Kasese	30.06	0.1	931	1964-2016	0.623	0.182	0.312	0.301
Masindi	31.43	1.41	1136	1960-2016	0.063	0.16	0.501	0.131
Kabale	29.6	-1.15	1743	1960-2016	0.085	0.34	0.887	0.271
Gitega	30.06	-1.95	1524	1970-2018	0.356	0.074	0.316	0.296
Nyagatare	30.31	-1.28	1366	1970-2018	0.343	0.036	0.298	0.066
Nyanza lac	29.62	-4.32	874	1970-2018	0.969	0.118	0.239	0.319
Gisenyi	29.26	-1.66	1591	1970-2018	0.65	0.072	0.495	0.491

Figures

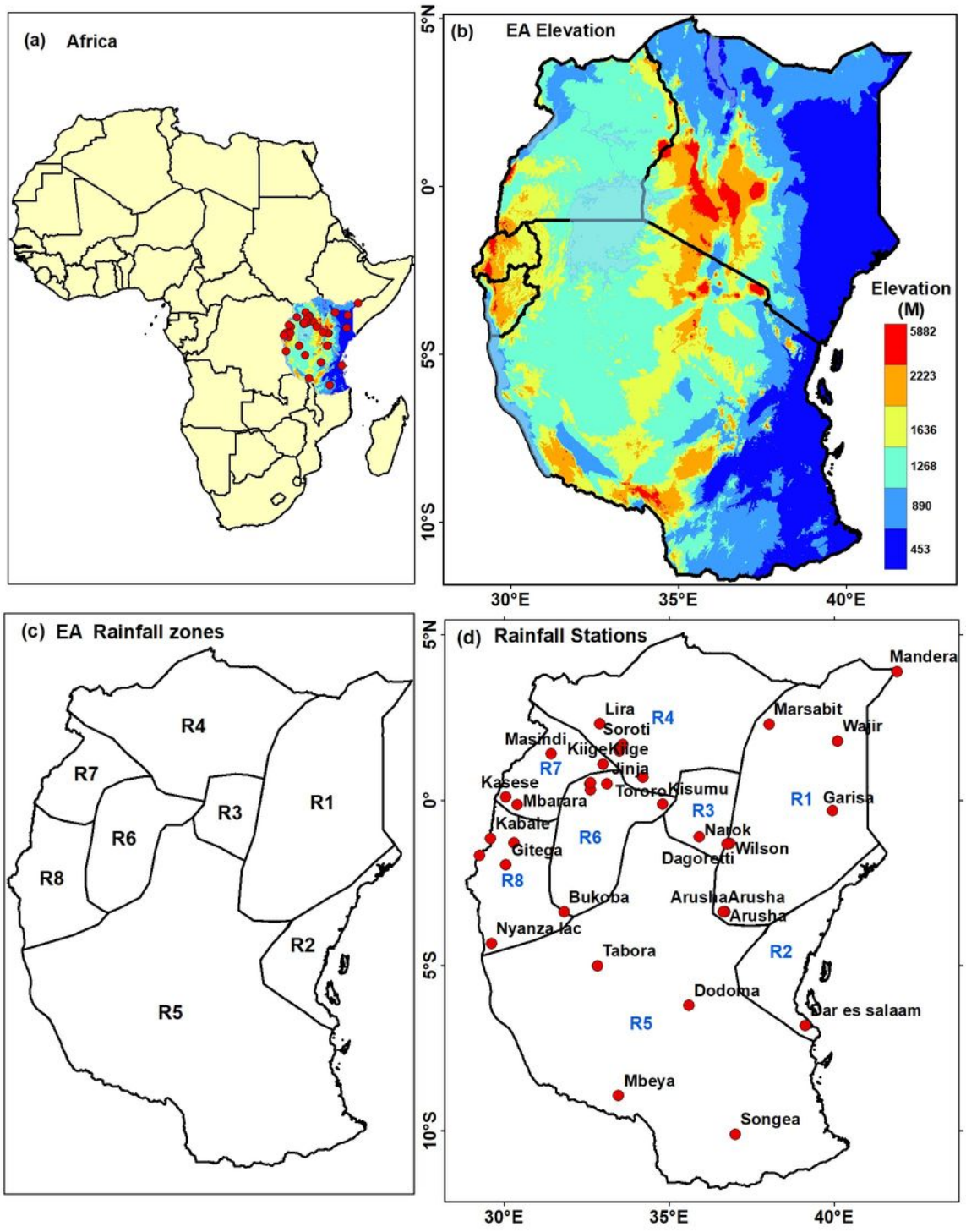

Figure 1

Shows map of Africa (a), showing East Africa right (b), and meteorological stations (red dots). Note: The designations employed and the presentation of the material on this map do not imply the expression of any opinion whatsoever on the part of Research Square concerning the legal status of any country,

territory, city or area or of its authorities, or concerning the delimitation of its frontiers or boundaries. This map has been provided by the authors.

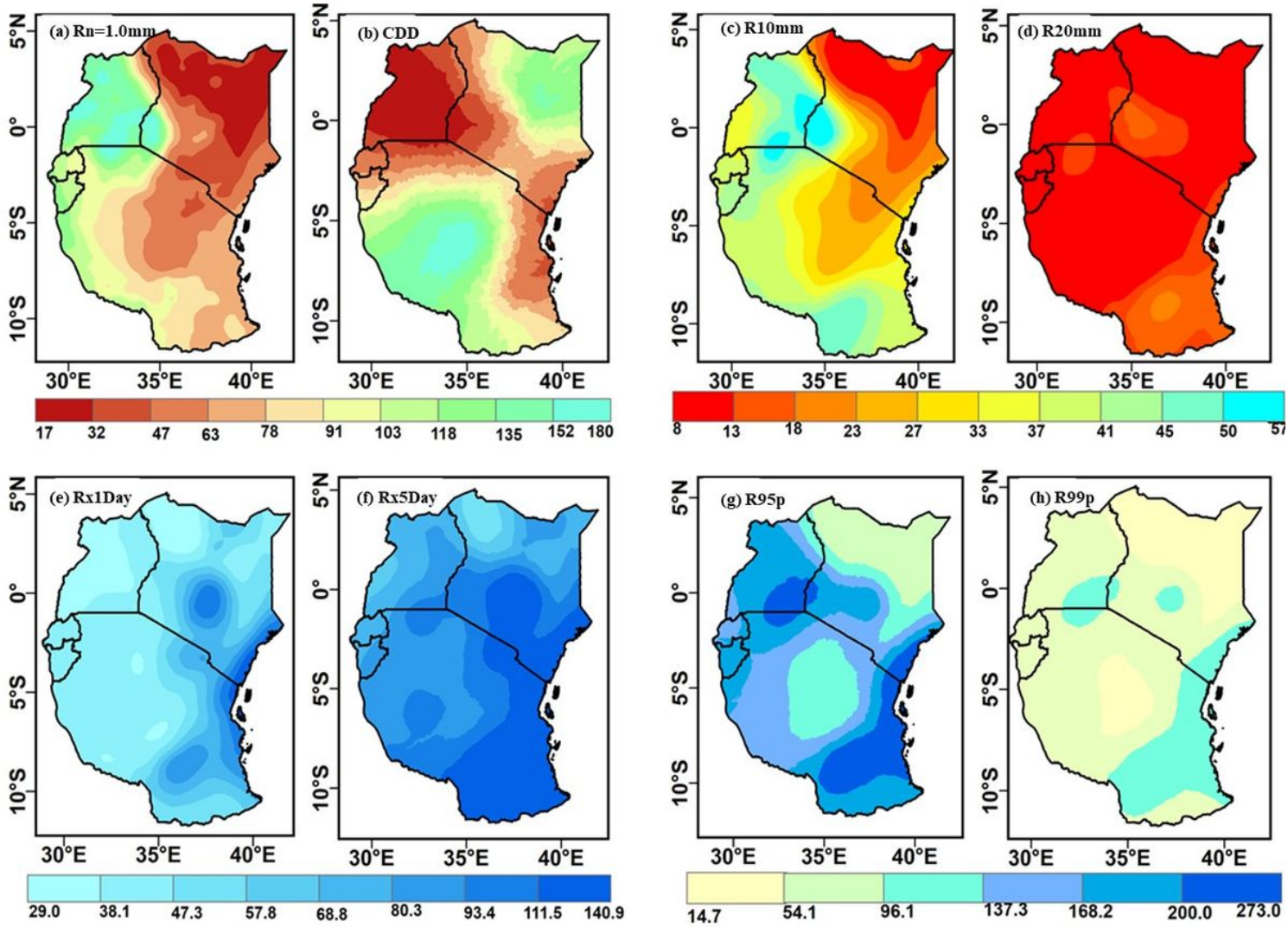

Figure 2

Shows the spatial distribution for the wet day (Rn=1.0mm(a), consecutive dry day CDD(b), the annual count of days when precipitation≥ 10mm(c), the annual count of days when precipitation≥ 20mm(d), max 5-day precipitation amount (RX1day) (e), 5-day precipitation amount (RX5day) (f), Very wet days R95p (g) and extremely wet days R95p (h) over East Africa during the period 1981-2017 Note: The designations employed and the presentation of the material on this map do not imply the expression of any opinion whatsoever on the part of Research Square concerning the legal status of any country, territory, city or area or of its authorities, or concerning the delimitation of its frontiers or boundaries. This map has been provided by the authors.

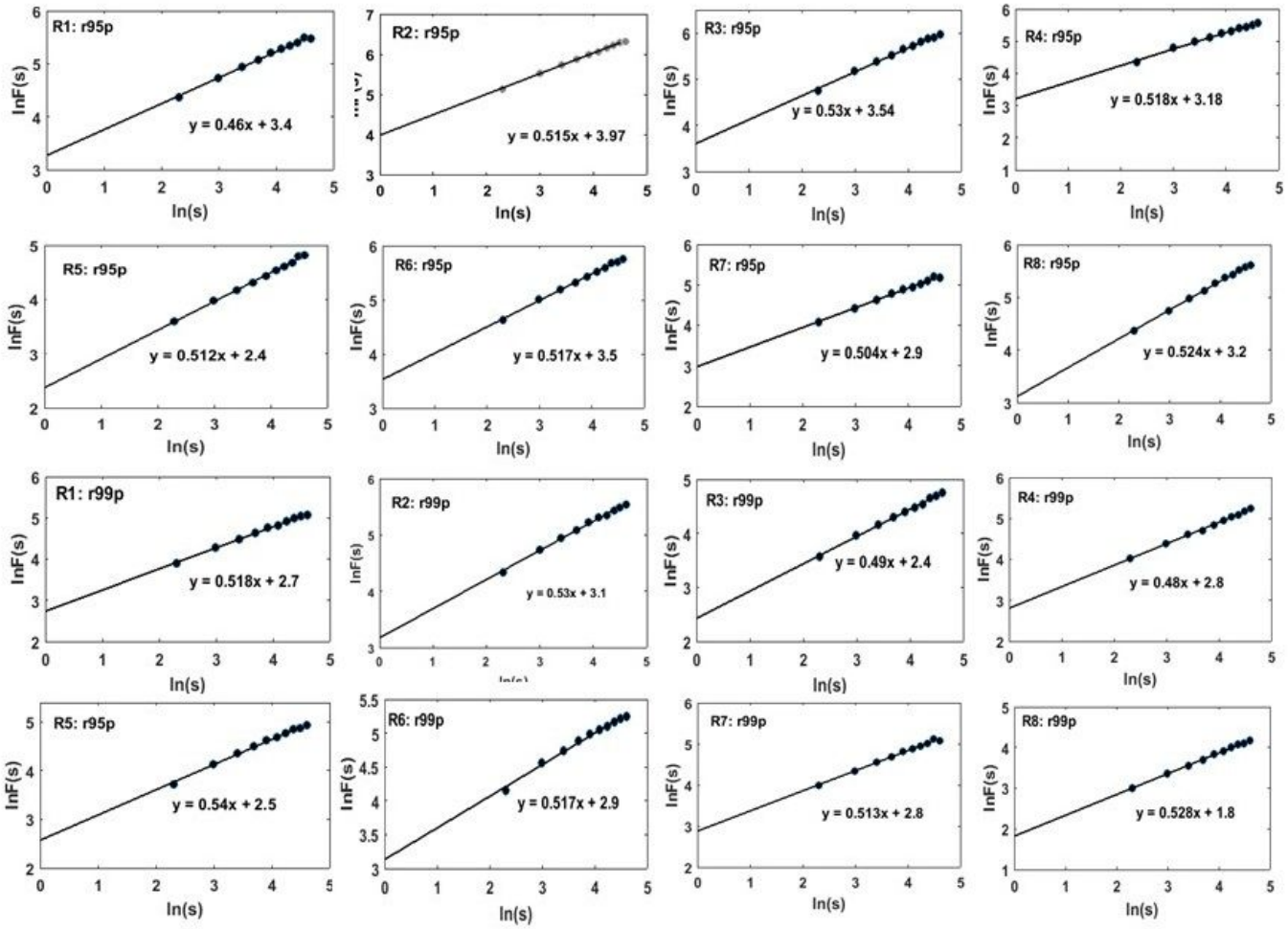

Figure 3

Shows Detrended Fluctuation Analysis (DFA) for long-range forecasting of extreme precipitation indices (r95p) and r99p for 8 rainfall zones (R1-R8) over East Africa.

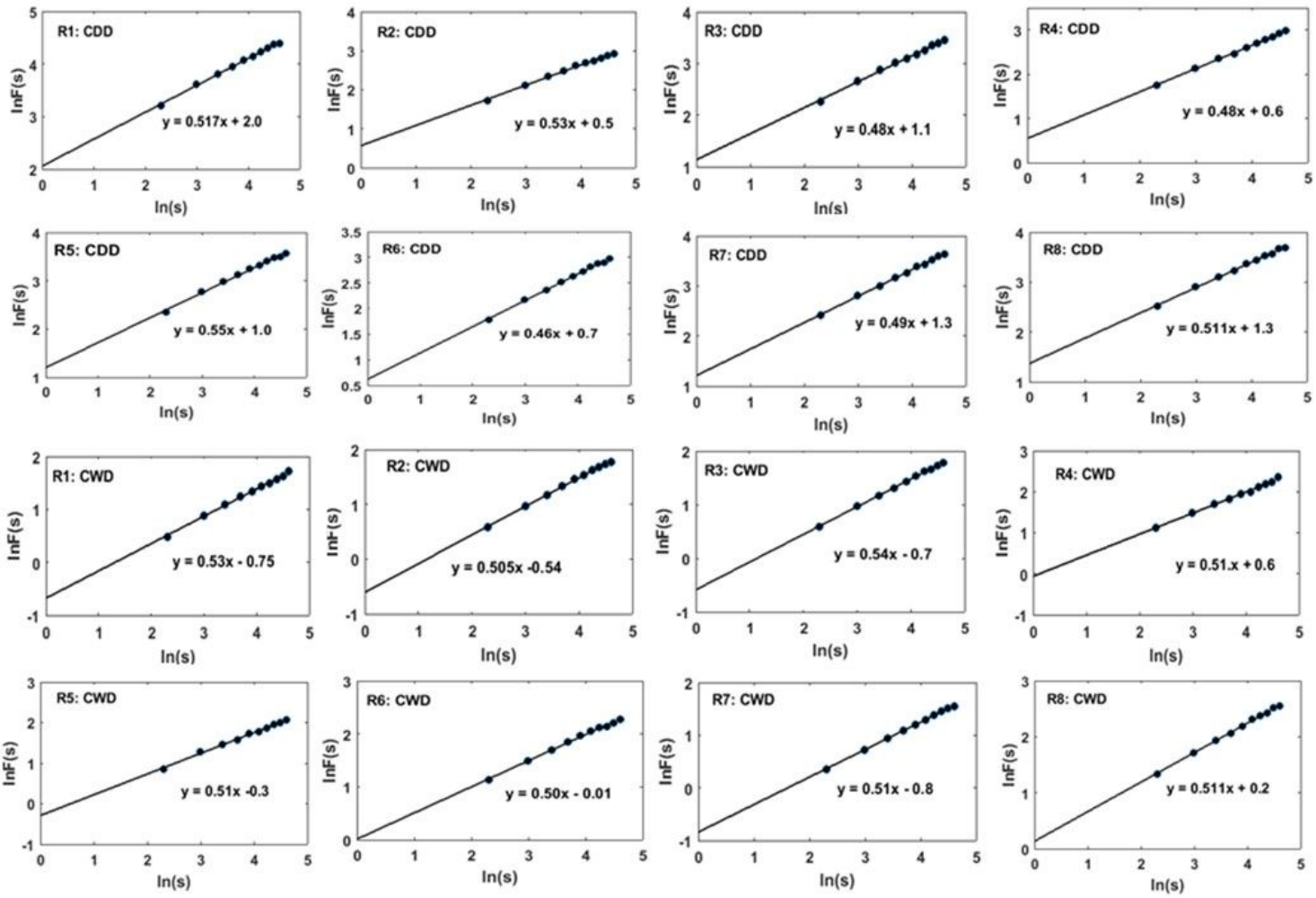

Figure 4

Detrended Fluctuation Analysis (DFA) for long-range forecasting of extreme precipitation indices CDD and CWD for 8 rainfall zones (R1-R over East Africa

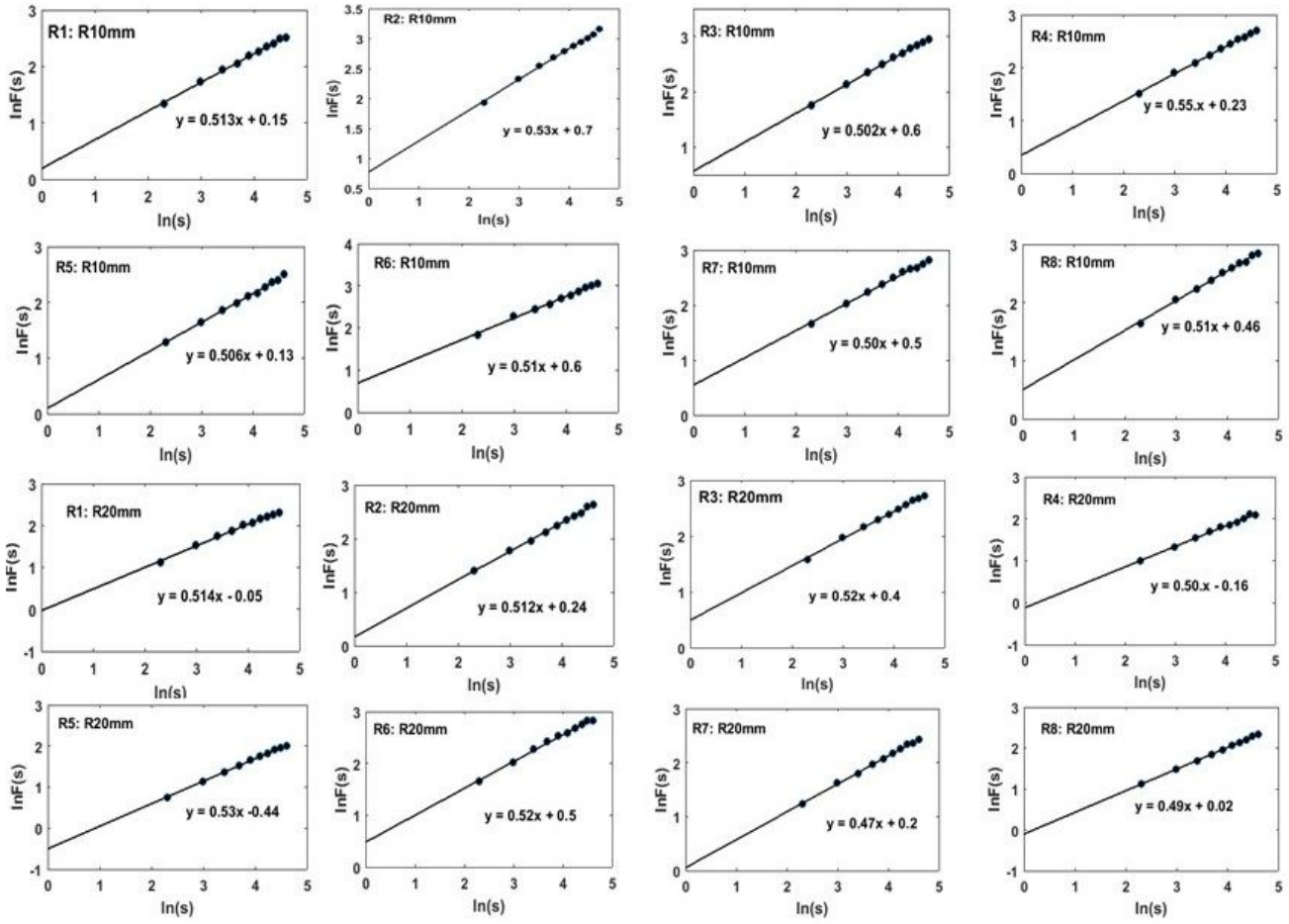

Figure 5

Detrended Fluctuation Analysis (DFA) for long-range forecasting of extreme precipitation indices R10mm and R20mm for 8 rainfall zone (R1-R) over East Africa.

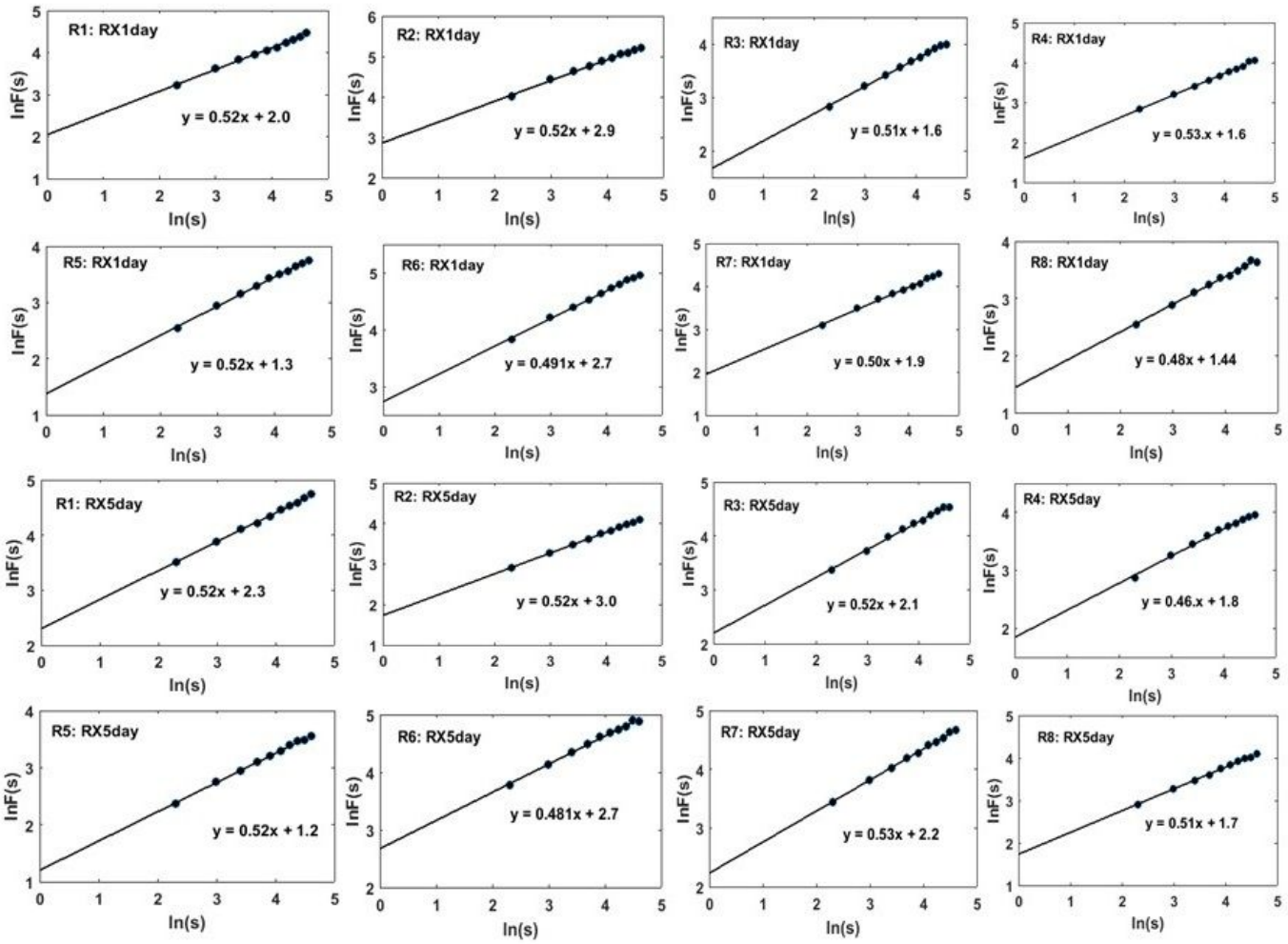

Figure 6

Detrended Fluctuation Analysis (DFA) curves for long-range forecasting of extreme precipitation indices RX1day and RX5 days for 8 rainfall zone (R1-R) over East Africa

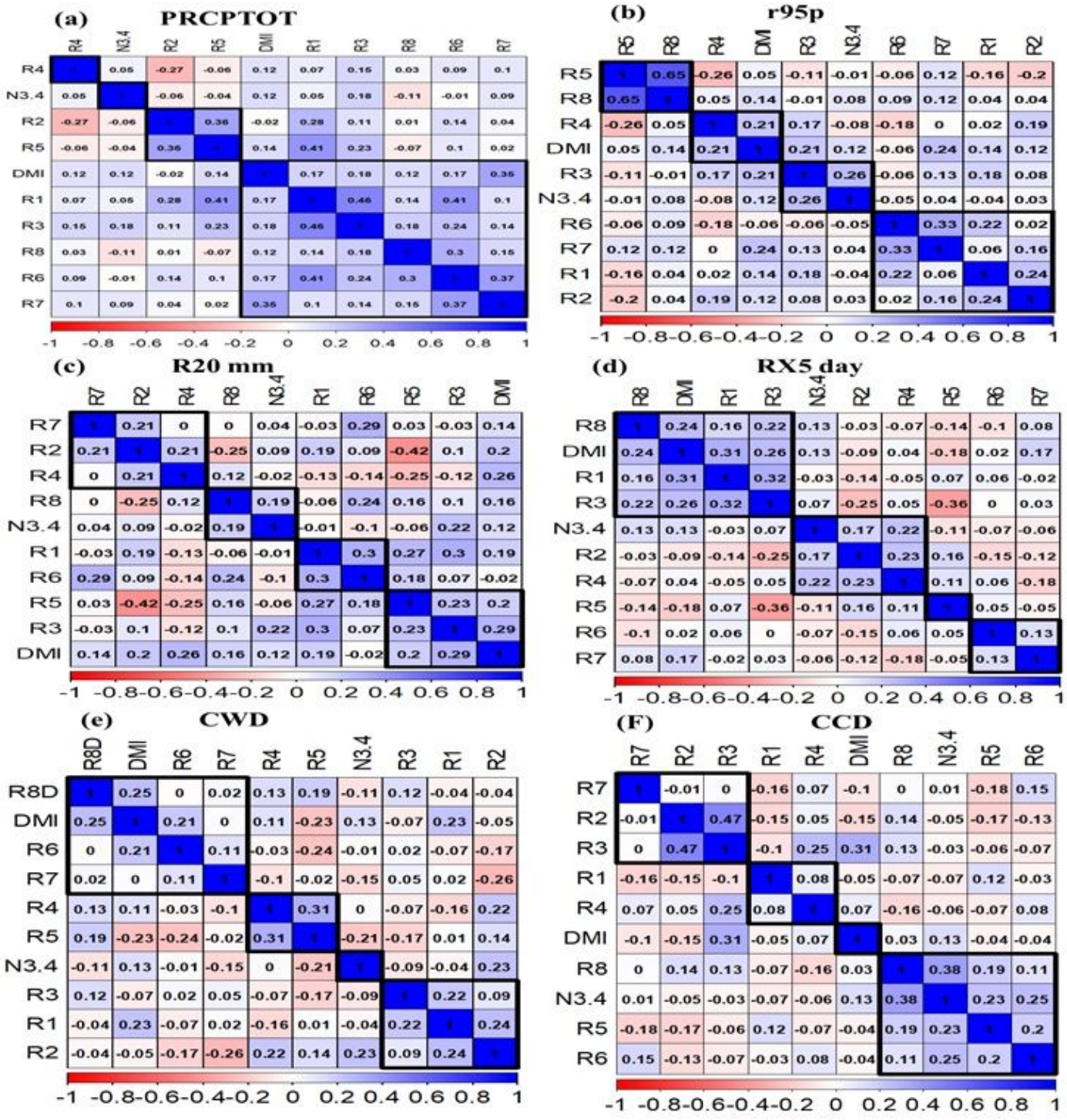

Figure 7

shows the correlations plots for annual total wet-day precipitation (PRCPTOT) (a), very heavy rainfall (r95p) (b), annual count of days when precipitation≥ 20mm(c), max 5-day precipitation amount (RX5day) (d), consecutive wet days (CWD) (e), consecutive dry days (CCD)(f). (Note DMI= Dipole Mode Index and N3.4 = Nino 3.4 index).